PS C23

Zinc regulation of an outwardly rectifying Cl^- conductance in mouse inner medullary collecting duct cells (mIMCD-3 cell-line)

J. Linley, M.A. Gray and N.L. Simmons

School of Cell and Molecular Biosciences, Medical School, Framlington Place, University of Newcastle upon Tyne, Newcastle upon Tyne NE2 4HH, UK

Zinc is present in normal urine and may retard calcium phosphate stone formation (Meyer & Angino, 1977). Our previous studies using renal inner medullary collecting duct cells (IMCD-3 cell-line) have identified the presence of a spontaneously active apical Cl^- conductance (Stewart *et al.* 2001) that is regulated by kinins, and external ATP via increased intracellular calcium ($[Ca^{2+}]_i$) (Stewart *et al.* 2001). Here we report stimulation of IMCD Cl^- conductance by extracellular Zn^{2+} via release of intracellular Ca^{2+}.

Cl^- currents were measured using the perforated (amphotericin 240 mg ml^{-1}) patch clamp whole cell recording configuration with a standard NaCl-rich bath solution and a KCl-rich pipette solution (Stewart *et al.* 2001).

Initial recordings with a holding potential of 0 mV with excursions to ± 60 mV gave outwardly rectifying time-independent currents (current densities ± 60 mV, 131 ± 14 pA pF^{-1}, −74 ± 8 pA pF^{-1} (means ± S.E.M.), $n = 6$) with an E_{rev} of –14.1 ± 2.8 mV. In the presence of 400 mM $ZnCl_2$ there was a progressive stimulation of current magnitude to a sustained plateau at 4–5 min, of 253 ± 31 pA pF^{-1} and −139 ± 18 pA pF^{-1} at ± 60 mV ($n = 6$), whilst E_{rev} shifted close to the Cl^- equilibrium potential (–6.5 ± 0.9 mV). The stimulated current was partially reversed on Zn^{2+} removal. In order to investigate whether extracellular Zn^{2+} stimulation of current density was a direct action, measurements of $[Ca^{2+}]_i$ were made using fura-2 loaded IMCD-3 cells. Superfusion of the standard Na^+-rich Krebs solution plus 400 mM $ZnCl_2$ resulted in a transient increase in $[Ca^{2+}]_i$, and/or a progressive increase in $[Ca^{2+}]_i$ that was partially reversible ($n = 9$). Superfusion of 400 mM $ZnCl_2$ in Ca^{2+}-free medium failed to abolish Zn^{2+}-induced increments in $[Ca^{2+}]_i$ ($n = 5$).

Since our previous studies have excluded the presence of the extracellular Ca^{2+}-sensing receptor in IMCD-3 cells (Stewart *et al.* 2001), these data suggest that a zinc-sensing receptor activates intracellular $[Ca^{2+}]_i$ so increasing Cl^- conductance in IMCD cells.

Meyer JL & Angino EE (1977). *Invest Urol* **14**, 347–350.

Stewart GS *et al.* (2001). *J Membr Biol* **180**, 49–64.

This work was supported by an NKRF studentship award to J.L.

PS C24

Effect of matrix extracellular phosphoglycoprotein on renal phosphate excretion in the rat

H. Dobbie* N. Faria† J.M. Slater† P.S.N. Rowe‡ D.G. Shirley* and R.J. Unwin*

**Department of Physiology, Royal Free and University College Medical School, Rowland Hill Street, London NW3 2PF, †Centre for Analytical Science, Birkbeck College, Malet Street, London WC1E 7HX, UK and ‡Department of Periodontics, University of Texas Health Science Center at San Antonio, TX, USA*

It has long been postulated that there are controls on renal phosphate handling in addition to the well-understood vitamin D/PTH axis. In oncogenic osteomalacia, patients have a tumour-related increase in urinary phosphate loss that resolves when the tumour is resected. Matrix extracellular phosphoglycoprotein (MEPE), a protein isolated from a patient with oncogenic osteomalacia (Rowe *et al.* 2000), is a candidate regulator of phosphate homeostasis. It is known to be synthesized by osteoblasts (Argiro *et al.* 2001) but its renal actions in intact animals are unclear.

Male Sprague-Dawley rats were anaesthetised with intraperitoneal sodium thiopentone (100 mg kg^{-1}), prepared for clearance studies and infused intravenously with 0.9% NaCl solution at 4 ml h^{-1}. After a 1 h control period the infusion was changed to include PTH (40 μg kg^{-1} h^{-1}) or MEPE (600 μg kg^{-1} h^{-1}), or continued as saline alone, for the following 2 h. Urine phosphate loss was measured hourly. Glomerular filtration rate was determined by clearance of tritiated inulin and blood pressure was measured continuously. At the end of the experiment the animal was humanely killed.

	Control period (μmol h^{-1})		Experimental period (μmol h^{-1})
Saline only	32 +/- 12	p=0.84	36 +/- 9
PTH	17 +/- 6	p=0.03	69 +/- 7
MEPE	22 +/- 7	p=0.03	57 +/- 5

Table 1. Urinary phosphate excretion in the control period and during the second hour of infusion with MEPE or PTH (experimental period). Values are means ± S.E.M., with 6 animals in each group. Results for the control and experimental period were compared by the Wilcoxon matched pairs test.

Differences in phosphate excretion between groups during the control period were not statistically significant (one-way ANOVA). Phosphate excretion was significantly increased in animals infused with either PTH or MEPE, but not in those infused with saline alone. There was a small, non-significant decline in GFR over time in all groups and also a slight decline in blood pressure, but no differences were seen between groups.

These results show that infusion of MEPE into intact rats causes phosphaturia. The mechanism of this effect and whether it may be of physiological as well as pathological significance remain to be determined.

Argiro L *et al.* (2001). *Genomics* **74**, 342–351.

Rowe PS *et al.* (2000). *Genomics* **67**, 54–68.

This work was supported by the National Kidney Research Fund. We thank Russ Blacher at Acologix for the supply of MEPE.

All procedures accord with current UK legislation

PS C25

Endogenous ATP concentrations in proximal convoluted tubules of the rat

R.M. Vekaria, R.J. Unwin and D.G. Shirley

Centre for Nephrology and Department of Physiology, Royal Free & University College Medical School, Royal Free Campus, London NW3 2PF, UK

Evidence is accumulating that extracellular nucleotides may play a role in the regulation of renal water and electrolyte excretion. Nucleotide (P2) receptors are present in both basolateral and apical membranes of renal tubules (Schwiebert & Kishore, 2001), and luminal application of exogenous ATP or its analogues has been found to modulate transport processes in proximal and distal nephron (M.A. Bailey, personal communication; Lehrmann *et al.* 2002). However, to date, no values for luminal concentrations of endogenous ATP *in vivo* have been reported, so the extent to which apical P2 receptors are activated under physiological conditions is unknown. In the present study we have therefore used micropuncture to collect fluid from rat proximal tubules in an attempt to quantify endogenous ATP.

Adult male Sprague-Dawley rats ($n = 7$) were anaesthetised with sodium thiopentone (LINK Pharmaceuticals; 100 mg kg^{-1}, I.P.) and prepared surgically for micropuncture of the left kidney. Sharpened glass micropipettes were used to collect fluid from mid-proximal convoluted tubules of superficial nephrons. Each collection lasted 4 min, and samples of the tubular fluid (80 nl) were then deposited in ice-cold water (50 μl) to halt ATP degradation; 10 such samples were pooled in the same diluent, then frozen prior to analysis. ATP concentration was measured using the luciferin–luciferase enzyme reaction (BioThema AB). An assessment was also made of soluble nucleotidase activity in proximal tubular fluid: ATP standard solutions (12 nl) were mixed (under oil) with 100 nl of tubular fluid; the reaction was stopped 5–40 min later. At the end of each experiment, the rat was killed with an overdose of anaesthetic.

In five pooled samples, the ATP concentration was 255 ± 20 nmol l^{-1} (mean ± S.E.M.). The half-life of ATP in mid-proximal tubular fluid was found to be 36 min (95% confidence intervals: 31–43 min) at room temperature.

Taking account of this evidence for soluble nucleotidases in tubular fluid, as well as the presence of ectonucleotidases in proximal tubular brush-border membranes (Vekaria *et al.* 2003), it is clear that the measured concentration of ATP represents a minimum value for endogenous ATP in the vicinity of the proximal tubular apical membrane. We suggest that this is consistent with a physiological role for luminal ATP in regulating proximal tubular function.

Lehrmann H *et al.* (2002). *J Am Soc Nephrol* **13**, 10–18.

Schwiebert EM & Kishore BK (2001). *Am J Physiol Renal Physiol* **280**, F945–963.

Vekaria RM *et al.* (2003). *3rd FEPS Congress 2003*, P07–22.

This work was supported by the National Kidney Research Fund and St Peter's Trust for Kidney, Bladder and Prostate Research.

All procedures accord with current UK legislation

PS C26

3-D reconstruction of the glomerular barrier and overlying podocyte reveals a sub-podocyte space: a new urinary space within the glomerulus?

C.R. Neal, S.J. Harper, D.O. Bates

Microvascular Research Laboratories, Department of Physiology, University of Bristol, Bristol BS2 8EJ, UK

The current understanding of glomerular ultrafiltration reveals that there is little resistance to flow after filtrate has traversed the glomerular basement membrane (GBM) and overlying slit diaphragms and entered the Bowman's space (BS). Fluid filters between the foot processes into BS or into the space between the glomerular parietal and visceral epithelial cells and the glomerular barrier.

We have reconstructed podocytes (visceral epithelial cells) and underlying GBM using micrographs of ultrathin (100 nm) serial sections of Wistar rat kidney (humanely killed by cervical dislocation) and human kidney (obtained at nephrectomy) with ethics committee approval and informed consent. In rat glomeruli an initial survey of the filtration barrier revealed that while the majority of filtration slits between foot processes open directly into the BS (66 ± 7%, mean ± S.E.M., range 20–80%), the remainder open into the space between the podocyte cell body and GBM. Full reconstruction of the podocyte and sub-podocyte space (SPS) showed that some processes which anchor the cell to the GBM form pores (0.6 ± 0.2 μm diameter, $n = 5$) which connect the SPS with BS. Other reconstructed podocyte pores form very narrow channels (0.16 ± 0.03 μm wide, $n = 6$) connecting the SPS to BS. The open area of the pores/channels connecting SPS to BS is 0.25–0.5% of the GBM area draining into the SPS. All the pore/channel openings onto the podocyte surface which have been fully reconstructed ($n = 5$) show that the pores/channels are transcellular − going through the podocytes not between neighbouring ones. Initial results on human glomeruli show similar findings.

The sub-podocyte space sandwiched between the podocyte and the GBM may enable more effective transduction of fluid flux by the podocyte and control of local ultrafiltration via podocytic pores and/or slit diaphragms. In addition, it is possible that the podocytic contractile state may exert an active control over the efflux of fluid from the filtration slits into the BS via the SPS. The functional significance of the SPS has yet to be determined.

This work was funded by The Wellcome Trust (58083) and B.H.F(BB2000003).

All procedures accord with current UK legislation, current local guidelines and the Declaration of Helsinki

PS C27

The mycotoxin ochratoxin A modulates paracellular permeability by removal of specific claudin isoforms from the tight junction

J. Mclaughlin, P.J. Padfield and C.A. O'Neill (introduced by Martin Steward)

Section of Gastrointestinal Sciences, University of Manchester Faculty of Medicine, Clinical Sciences Building, Hope Hospital, Salford M6 8HD, UK

On interaction with the intestine, the mycotoxin ochratoxin A (Maresca *et al.* 2001) is known to cause rapid inflammation,

diarrhoea and increased bacterial translocation. All these effects are consistent with a decrease in epithelial barrier function, but this has not been shown directly. In this study we demonstrated that ochratoxin A is able to reduce the barrier properties of the model intestinal cell line CaCO-2.

CaCO-2 cells were seeded on Transwell cell culture inserts with a mean pore size of 0.4 μM (Costar) at 3×10^5 cells cm^{-2} and were grown for 21 days or until the transepithelial electrical resistance (TER) had become stable. TER was monitored using an Evometer (World Precision Instruments) fitted with Chopstick electrodes. TER was normalised by the area of the monolayer and the background TER of blank filters was subtracted from the TER of the cell monolayer. Permeability measurements were made using membrane-impermeant FITC-dextrans. Dextrans were added to the apical chamber and basal chamber fluid collected after 4 h incubation and analysed using a fluorimeter. Tight junction protein constituents were analysed by immunoblotting. Statistical analysis was performed using the non-parametric Mann-Whitney test. Values given are means ± standard deviation.

We monitored the TER of CaCO-2 cells growing in the presence or absence of ochratoxin A over 24 h. In untreated cells the TER remains stable over this time course at around 3200–3300 Ω cm^2 When ochratoxin A was added to either the apical or basolateral chamber, the transepithelial resistance of CaCO-2 monolayers reduced by approximately 40 % (± 6 %) in 24 h, with significant differences between control and treated cells observed as early as 4 h post-treatment ($P < 0.04$, $n = 6$). At the same time, the permeability of the monolayer increased by approximately 2.5-fold with respect to 4 and 10 kDa FITC dextrans. In contrast no change in the permeability of either 20 or 40 kDa dextran ($n = 5$) was observed. When tight junction protein constituents were analysed by immunoblotting, a reduction in the levels of claudin isoforms 3 and 4, but not 1 was observed.

These results suggest that ochratoxin A is able to modulate the paracellular pathway in CaCO-2 cells by removal of specific claudin isoforms.

Maresca M *et al.* (2001). *J Tox Appl Pharm* **176**, 54–63.

This work was funded by the Digestive Diseases Foundation

PS C28

ATP-promoted release of $Co(NH_3)_4$ATP occluded in pig kidney Na^+,K^+-ATPase reveals negative co-operativity between two ATP sites

D.G. Ward, W. Schoner* and J.D. Cavieres

*Department of Cell Physiology & Pharmacology, University of Leicester, Leicester LE1 9HN, UK and * Institute of Biochemistry and Endocrinology, Justus-Liebig-University Giessen, D-35392 Giessen, Germany*

$Co(NH_3)_4$ATP has been used to probe ATP binding sites in the sodium pump. The purified enzyme (Jørgensen, 1974) binds the analogue at two sites, with $K_D = 0.1$ μM and 0.4–0.6 mM (Scheiner-Bobis *et al.* 1987; Ward & Cavieres, 2003). At the latter, binding is followed by slow non-covalent trapping and inactivation of the K^+-dependent reactions of the pump cycle. We have reported (Ward *et al.* 1997) that low concentrations of ATP and ATP analogues like $Co(NH_3)_4$ATP itself promote the release of the occluded [^{3}H]- or [γ^{33}P]-labelled $Co(NH_3)_4$ATP. The time courses fit the sum of two decaying exponentials. At 20°C, the amplitude for the fast exponential increases hyperbolically with the ATP concentration, with $K_{0.5} = 3.4$ μM, and $1/\tau$ for the slow exponential increases with $K_{0.5} = 1.9$ μM. This indicates that ATP binds to the $Co(NH_3)_4$ATP-occluded enzyme and accelerates a slow deocclusion reaction; the released analogue would then bind back to the pump at equilibrium, with a very high affinity, and under ATP competition.

The high-affinity rebinding was exposed by passive dilution of the suspension of $Co(NH_3)_4$[^{3}H]ATP-enzyme (no nucleotide added), as this caused $Co(NH_3)_4$[^{3}H]ATP release; we estimated $K_D = 11$ nM from the mass action. Alternatively, we released $Co(NH_3)_4$[^{3}H]ATP with ATP and removed the latter on DEAE-Sephadex. When we presented the released analogue to the washed depleted enzyme (still 'K^+-inactive'), we estimated $K_D = 26$ nM. With the native Na^+,K^+-ATPase instead, K_D was 70 nM, not too different from the high affinity towards fresh analogue. The partially inactivated, depleted pump could also bind [γ^{33}P]ATP and fresh $Co(NH_3)_4$[^{3}H]-ATP with K_D values of 330 and 450 nM, respectively.

These results suggest that ATP and other nucleotides bind at the extant high affinity site of the $Co(NH_3)_4$ATP-enzyme, promoting $Co(NH_3)_4$ATP deocclusion and a decrease of $Co(NH_3)_4$ATP rebinding affinity at the modified regulatory site. By extension, these findings imply that negative co-operativity between the two ATP sites plays an important role in the reaction of native Na^+,K^+-ATPase.

Jørgensen PL (1974). *Biochim Biophys Acta* **356**, 36–52.

Scheiner-Bobis G *et al.* (1987). *Eur J Biochem* **168**, 123–131.

Ward DG & Cavieres JD (2003). *J Biol Chem* **278**, 14688–14697.

Ward DG *et al.* (1997). *J Physiol* **499.P**, 25–26*P*.

This work was supported by research grants from The Wellcome Trust and the Medical Research Council.

PS C29

Effect of endocytosis inhibitors on the uptake of TTR/T4 complex in rabbits

N.A. Kassem, A. Patel, M.H. Paywandi and M.B. Segal

Centre for Neurosciences Research, King's College London, St Thomas' Campus, London SE1 7EH, UK

It has been shown that transthyretin (TTR), which is synthesised and secreted by the choroid plexus (CP), binds avidly to thyroxine (T4) and might be responsible for the concentration of T4 being higher in the CSF than plasma (Schreiber *et al.* 2001). We have shown in a previous study that TTR when complexed with T4 increases the uptake of T4 into brain tissues (Kassem *et al.* 2002), but at the cellular level the mechanism by which this protein complex enters the brain is not clear. Kuchler-Bopp *et al.* (2000) have demonstrated that the TTR receptors are expressed on ependymoma cells and it has been suggested that the ependyma may act as a reservoir for T4.

By using the ventriculo-cisternal perfusion (VC) technique in anaesthetized rabbits (Domitor and pentobarbitone given I.V. at a dose of 0.5 mg and 10 mg kg^{-1}, respectively; at the end of the experiment the animals were humanely killed), we have investigated the effect of endocytosis inhibitors on the brain uptake and loss of TTR as ^{125}I-TTR–T4 complex from the aCSF perfusate. Values are means ± S.E.M., and were compared with Student's unpaired *t* test.

Nocodazole at 50 μM was added to the aCSF perfusate and the uptake of TTR–T4 complex into the caudate nucleus was significantly reduced from a control value of 49.2 ± 8.6 ml (100 g)$^{-1}$, to 23.0 ± 9.7 ml (100 g)$^{-1}$ ($P < 0.05$,

$n = 3$). In the ependymal layer (EL) the control uptake was 38.6 ± 5.8 ml (100 g)$^{-1}$ ($n = 5$), while in the presence of nocodazole the uptake was significantly decreased to 6.9 ± 3.4 ml (100 g)$^{-1}$ ($P < 0.01$, $n = 3$). Similarly after the addition of 100 μM monensin to the aCSF, the uptake of the TTR–T4 complex into EL was reduced by 38.5 ± 7.0 ml (100 g)$^{-1}$ ($P < 0.05$, $n = 3$), a significant difference from the control. However both drugs had no effect on the loss of the complex from the aCSF.

We conclude that the uptake of TTR–T4 complex from the aCSF into brain is by a receptor-mediated endocytosis.

Kassem NA *et al.* (2002). *J Physiol* **543.P**, 17*P*.

Kuchler-Bopp S *et al.* (2000). *J Physiol* **570**, 185–194.

Schreiber G *et al.* (2001). *Micros Res Tech* **52**, 21–30.

This work was partly funded by Al-Tajir World of Islam Trust.

All procedures accord with current UK legislation

PS C30

RNA interference reveals distinct roles for plasma membrane syntaxins in epithelial fluid secretion

Ross K.J. McLennan*†, S.A. Davies*, G.W. Gould† and J.A.T. Dow*

**Division of Molecular Genetics and Henry Wellcome Laboratory of Cell Biology and †Division of Biochemistry and Molecular Biology, University of Glasgow, Glasgow, UK*

One of the key events in intracellular vesicle trafficking is the fusion of the vesicle membrane with the membrane of its target organelle or compartment. At the core of every pairing between vesicle and target membrane lies the interaction between SNARE proteins, and every SNARE-dependent fusion event involves a member of the syntaxin family. By utilizing the model organism *Drosophila melanogaster*, it is possible to dissect syntaxin functions in a fully differentiated context.

We have identified 10 members of the *Drosophila* syntaxin family *in silico*, and shown that all 10 syntaxins are expressed at all developmental stages and in all adult tissues studied. This is a smaller family than found in mammalian systems, but is still predicted to be sufficient to direct targeted vesicle trafficking. Immunocytochemical analysis has revealed that each of these syntaxins has a unique and distinct subcellular distribution, although certain family members are only expressed in a subset of cell types within the Malpighian tubule – a model, polarized epithelium (Dow & Davies, 2003). This represents the first detailed characterisation of syntaxin expression in a single cell type in higher eukaryotes.

Two syntaxins (Syx1A and Syx4) were shown to be localised exclusively to the plasma membrane of tubule cells, with Syx1A found only at the apical membrane and Syx4 solely in basolateral domains. We analysed the function of each of these syntaxins by utilising the power of *Drosophila* genetics (in particular the UAS:GAL4 binary expression system) and RNA interference to knock-down the expression levels of each protein in a cell-specific manner.

Our results show that the plasma membrane syntaxins are involved in the regulation of different steps of the fluid secretion phenotype of this model tissue. Syx1A plays a role in regulating the activity of the apical V-ATPase by mediating the trafficking of components of the V1 subunit. Whilst preliminary data show that Syx4 plays a role in the trafficking of SOC channels to the basolateral membrane in response to the emptying of internal Ca^{2+} stores.

In addition, transgenic *Drosophila*, in which Syx4-RNAi expression is driven in specific cells of the Malpighian tubule (and Syx4 function is thus reduced), show an extreme reduction in their ability to survive infection with Gram-negative bacteria. Subsequent work has shown that isolated Malpighian tubules expressing the Syx4-RNAi construct have a reduced ability to either detect the presence of bacteria or to mount a secreted response.

Dow JAT & Davies SAD (2003). *Physiol Reviews* **83**, 687–729.

This work was supported by the Wellcome Trust and the BBSRC.

PS C31

The role of uterine glands in fluid absorption in the peri-implantation period

Naguib Salleh, Stuart R. Milligan and Richard J. Naftalin

Division of Physiology, King's College, Guy's Campus, London SE1 1UL, UK

Implantation requires synchronisation between blastocyst development and the transformation of the endometrium into a receptive state. During this period the uterus undergoes 'closure' with a complete loss of uterine fluid resulting in sandwiching of the blastocyst between the opposing uterine walls, thus initiating contact between blastocyst and the endometrium. The mechanism underlying fluid loss is currently thought to be associated with changes in Na^+ absorption. This may involve changes in the expression of epithelial sodium channel transporter (ENaC) and cystic fibrosis transmembrane regulator (CFTR) in the uterine glandular epithelium (Chan *et al.* 2002). This view is supported by *in vitro* observation of amiloride-sensitive fluid absorption in the uterine glands of progesterone-treated rats (Naftalin *et al.* 2002). The current study extends this result to fluid absorption *in vivo*.

These experiments were performed in ovariectomised Wistar rats treated with steroids to mimic events in early pregnancy. The rats were divided into three groups ($n = 6$ per group): a control group receiving vehicle injection only; 3 days of 0.2 mg oestradiol treatment; or 3 days 0.2 mg oestradiol treatment followed by 3 days 4 mg progesterone treatment. The rats were anaesthetised with intraperitoneal injection of 0.1 ml ketamine and 0.15 ml xylazine HCl. Fluid absorption rates from the uterine horns were monitored by weight changes between inflow and outflow of uterine luminal perfusate and the concurrent changes in the effluent concentration of non-absorbable fluorescein(F)-dextran (molecular mass 450 kDa). The rats were humanely killed by cervical dislocation. ENaC and CFTR distribution was studied in fixed tissues using specific fluorescent antibodies and confocal microscopy.

Progesterone treatment resulted in an increased rate of fluid absorption which was reversed by amiloride, as evidenced by net changes in perfusate volume and increases in F-dextran concentration. Oestradiol treatment resulted in a small net secretion. ENaC was predominantly distributed around the glandular lumen in the progesterone-treated rats, whilst being absent in the oestradiol-treated and control animals. CFTR, however, was predominantly distributed around the glands in oestradiol-treated and less in progesterone-treated and control animals.

These observations suggest that progesterone upregulates ENaC in the uterine glands resulting in increased sodium absorption from the luminal fluid which may contribute to uterine closure.

Chan LN *et al.* (2002). *J Membr Biol* **185**, 165–176.
Naftalin RJ *et al.* (2002). *Reproduction* **123**, 633–638.

All procedures accord with current UK legislation

PS C32

cGMP/PKG II-dependent inhibition of a pH-dependent Zn^{2+}-evoked electrogenic transport pathway in human intestinal Caco-2 epithelia

Derek A. Scott*, Harry J. McArdle† and Gordon T.A. McEwan*

** Department of Biomedical Sciences, Institute of Medical Sciences, University of Aberdeen, Aberdeen AB25 2ZD and † Rowett Research Institute, Greenburn Road, Aberdeen AB21 9SB, UK*

Apical exposure to Zn^{2+} stimulates an inward short circuit current (I_{SC}) in Caco-2 epithelia (Scott *et al.* 2003). This transport process is pH dependent, consistent with H^+-coupled uptake of Zn^{2+} across the apical membrane (Fleet *et al.* 1993). The present study set out to investigate intracellular regulation of Zn^{2+}-evoked electrogenic transport by cGMP.

I_{SC} determinations were made on voltage-clamped Caco-2 epithelia, grown on permeable supports (Anotec, Nunc). Cells were bathed with isotonic mannitol–Hepes buffer (37 °C; pH 7.4). At the onset of the experiment, apical pH was adjusted to 6.0. Zinc-histidine (1:5 molar ratio) was applied apically. The cGMP analogue 8-Br-cGMP (100 μM) was applied to the apical bathing medium for 20 min prior to Zn^{2+} exposure. In experiments investigating the effects of staurosporine (0.5 μM), H-89 (50 μM), chelerthryne chloride (20 μM) and Rp-8-pCPT-cGMPs (20 μM), these were applied 30 min prior to 8-Br-cGMP.

Exposure to 8-Br-cGMP reversed Zn^{2+}-induced inward I_{SC} to a small, but significant ($P < 0.05$, Student's unpaired t test), outward I_{SC} at all Zn^{2+} concentrations tested (25–1000 μM). Staurosporine reversed cGMP-induced inhibition of Zn^{2+}-evoked I_{SC}, resulting in an inward I_{SC} (control $V_{max} = 0.73 \pm 0.08$ μA cm^{-2} (5); stauro + 8-Br-cGMP $V_{max} = 0.37 \pm 0.03$ μA cm^{-2} (4) (means ± S.E.M. (n)). Staurosporine alone stimulated the Zn^{2+}-induced I_{SC} with V_{max} rising ($P < 0.05$ *vs.* control) to 1.79 ± 0.10 μA cm^{-2} (8). The PKG II inhibitor, Rp-8-pCPT-cGMPs, also abolished the inhibitory action of 8-Br-cGMP on Zn^{2+}-induced I_{SC} (control $V_{max} = 0.61 \pm 0.09$ μA cm^{-2} (5); Rp-8-pCPT-cGMPs + 8-Br-cGMP $V_{max} = 1.20 \pm 0.08$ μA cm^{-2} (4)). Rp-8-pCPT-cGMPs alone stimulated the Zn^{2+}-induced I_{SC}, V_{max} rising ($P < 0.01$) to 1.39 ± 0.19 μA cm^{-2} (4). Neither the PKA inhibitor, H89, nor the PKC inhibitor, chelerthryne chloride, had any effect on the actions of 8Br-cGMP or on the Zn^{2+}-evoked I_{SC}.

These data demonstrate that the pH-dependent inward I_{SC}, induced by apical Zn^{2+} exposure in Caco-2 cells, was inhibited by intracellular cGMP. This inhibition was dependent on PKG II but not PKA or PKC. It has yet to be established whether the Zn^{2+}-evoked I_{SC} reflects Zn^{2+} transport *per se*. However, these results may suggest an important regulatory pathway for Zn^{2+} absorption in the small intestine.

Fleet JC *et al.* (1993). *Am J Physiol* **264**, G1037–1045.
Scott DA *et al.* (2003). *J Physiol* **547P**, *PC*61.

D.A.S. was supported by a BBSRC PhD studentship.

PS P106

Comparison of renal function in young and adult, anaesthetised New Zealand genetically hypertensive rats

Nick Ashton*, Philip Kelly† and Janet M. Ledingham†

** School of Biological Sciences, University of Manchester, Manchester, UK and † Department of Pharmacology, University of Otago, Dunedin, New Zealand*

Despite structural narrowing of the renal afferent arterioles (Ledingham *et al.* 1998), adult genetically hypertensive (GH) rats have been shown to have lower extracellular fluid volume and total body sodium similar to that of control normotensive (N) rats (Gresson *et al.* 1973). This normalisation of body fluid status may reflect renal compensation in the face of chronic exposure to high blood pressure. Accordingly, the aim of this study was to compare renal function in young and adult GH rats.

Standard renal clearance techniques were used to assess renal function in pentobarbitone-anaesthetised N and GH rats at the age of 5–6 weeks (N $n = 9$, GH $n = 5$) and 19–20 weeks (N $n = 6$, GH $n = 5$). Saline at 0.9 % containing inulin and para-aminohippuric acid was infused at 50 μl min^{-1} (100 g body wt)$^{-1}$ in young rats and 100 μl min^{-1} in adult rats for 3 and 6 h, respectively. Clearance measurements were made over the final hour in young rats and over 3 h in the adult rats. Animals were humanely killed at the end of the experiment.

	ERBF ml min^{-1}	GFR ml min^{-1}	UV µl min^{-1}	$U_{Na}V$ µmol min^{-1}
Young N	6.5 ± 0.9	1.1 ± 0.2	31.9 ± 7.7	4.7 ± 0.8
Young GH	*4.7 ± 0.5	*0.5 ± 0.06	*11.7 ± 1.9	*1.8 ± 0.6
Adult N	5.9 ± 0.9	1.2 ± 0.2	7.1 ± 2.5	0.3 ± 0.2
Adult GH	4.1 ± 0.3	1.0 ± 0.1	7.9 ± 2.2	0.3 ± 0.1

Table 1. Effective renal blood flow (ERBF), glomerular filtration rate (GFR), urine flow rate (*UV*) and sodium excretion ($U_{Na}V$) in young and adult N and GH rats. Values are means ± S.E.M. corrected to 100 g body weight. * $P < 0.05$ young N *vs.* GH, unpaired *t* test.

Blood pressure was significantly higher in both young (N 101 ± 6 *vs.* GH 125 ± 9 mmHg, Student's unpaired *t* test, $P < 0.05$) and adult GH rats (N 103 ± 7 *vs.* GH 149 ± 12 mmHg, $P < 0.01$). Young GH rats had significantly lower ($P < 0.05$) effective renal blood flow, glomerular filtration rate, urine flow rate and sodium excretion than N rats (Table 1). These differences were no longer apparent in adult rats.

Renal function is impaired in young but not adult GH rats. These data suggest that a shift in the pressure–natriuresis relationship occurs as the GH rat matures, resulting in the restoration of renal function at the expense of an increase in systemic blood pressure. Thus, impaired renal function may underlie the development of hypertension in the GH rat.

Gresson CR *et al.* (1973). *Clin Sci* **44**, 349–358.

Ledingham JM *et al.* (1998). *J Hypertens* **16**, 1945–1952.

This work was supported by a Wellcome Trust Travel Award.

All procedures accord with current UK legislation

PS P107

Effects of single bolus urotensin II injection on renal function in anaesthetised rats

Weihua Song, Nick Ashton and Richard J. Balment

School of Biological Sciences, University of Manchester, Manchester M13 9PT, UK

The peptide hormone urotensin II (UII) and its receptor GPR-14 have recently been identified in mammalian species, including man. Subsequent pharmacological studies have described profound cardiovascular and renal effects, suggesting a potential role in related disease states.

In the current study, anaesthetised (Intraval, 100 mg kg^{-1}) Sprague-Dawley rats ($n = 8$ per group) were infused with 0.9 % saline (containing [^{3}H]inulin as a marker of glomerular filtration rate (GFR) and para-aminohippuric acid as a marker of effective renal plasma flow) for 4 h prior to a single I.V. bolus injection of rat UII (10^{-10}–10^{-9} M) or vehicle (0.9 % saline). Previous studies in our laboratory have shown significant changes in cardiofunction at 10^{-9} M but not at 10^{-10} M. Saline infusion lasted for a further 2 h. Urine samples were taken every 15 min and blood samples were taken in the middle of each hour. Blood pressure was monitored throughout. Plasma and urine electrolyte concentrations were measured. Animals were humanely killed at the end of the experiment.

Change from 15 min before UII to 15 min after UII	10^{-9}M (%, n=8)	10^{-10}M (%, n=8)	Control (%, n=8)
GFR	-39.8 ± 9.6*	-25.4 ± 5.9*	-4.3 ± 9.2
UV	-36.3 ± 9.1*	-29.4 ± 4.8*	0.9 ± 0.9
ERBF	-43.4 ± 9.6*	-19.2 ± 5.4	-4.0 ± 7.3
FF	43.0 ± 24.4*	-6.9 ± 5.3	10.1±7.6

Table 1. Change (%) in glomerular filtration rate (GFR), urine flow rate (*UV*), effective renal blood flow (ERBF) and filtration fraction (FF) following I.V. injection of rat UII at either 10^{-9} or 10^{-10} M. Data are means ± S.E.M. *$P < 0.05$ 10^{-9} M group or 10^{-10} M group *vs.* control group, one-way ANOVA.

All measured variables were in a steady state and did not differ between groups prior to injection of UII. Compared with values in the 15 min collection period prior to injection, UII at both 10^{-10} and 10^{-9} M caused significant ($P < 0.05$) dose-dependent decreases in GFR and urine flow rate in the 15 min after injection (Table 1). UII at 10^{-9} M also produced a significant ($P < 0.05$) reduction in effective renal blood flow and an increase in filtration fraction. Significant decreases in urinary Na^+, K^+, Ca^{2+} and Mg^{2+} clearance and excretion were also observed. There was no significant change in mean arterial blood pressure.

These data show that UII is able to exert profound effects on renal haemodynamic function and support the suggestion that UII may play a role in regulating cardiovascular and renal function.

All procedures accord with current UK legislation

PS P108

A carboxy-terminal valine influences endocytosis of the ROMK2 potassium channel in *Xenopus laevis* oocytes

S. Hajihashemi*, G.J. Cooper* and S.J. White†

** Department of Biomedical Science, University of Sheffield, Sheffield S10 2TN, UK and † School of Biomedical Sciences, University of Leeds, Leeds LS2 9JT, UK*

Several studies have shown that C-terminal internalization motifs within ROMK (Kir1.1) channels are involved in clathrin-dependent endocytosis of ROMK from the plasma membrane of *Xenopus laevis* oocytes and rat cortical collecting duct (Moral *et al.* 2001; Zeng *et al.* 2002). We tested the involvement of valine 364, which lies within a type I PDZ-domain (EVDETDDQM) of rat ROMK2 by comparing endocytotic removal of wild-type EGFP-tagged ROMK2 (EROMK2) with a mutant ($EROMK2_{V364D}$) in which V364 was replaced by aspartate via site-directed mutagenesis.

Stage V and VI oocytes isolated from humanely killed *Xenopus laevis* ($n = 3$) were injected with 50 nl H_2O containing 1 ng (0.02 ng nl^{-1}) of cRNA encoding EROMK2 or $EROMK2_{V364D}$ and incubated at 18 °C for 3 days. Then half the oocytes in each group were exposed continuously to 25 μM brefeldin-A (BFA), an inhibitor of protein trafficking to the plasma membrane. Following addition of BFA, function of EROMK2 and $EROMK2_{V364D}$ (in −BFA ($n = 13$–15) and +BFA ($n = 13$–20) oocytes) was determined in the presence or absence of 5 mM $BaCl_2$ at an external $[K^+]$ of 2.00 mM by two-microelectrode voltage clamp. Membrane potential (V_m) and Ba^{2+}-sensitive current (I_K) are given as means ± S.E.M. and statistical significance (by ANOVA and Tukey's test) was taken at $P < 0.05$.

	EROMK2 + BFA		$EROMK2_{V364D}$ + BFA	
t (hours)	V_m (mV)	I_K (μA)	V_m (mV)	I_K(μA)
0	-95.6 ± 0.9	0.95 ± 0.07	-96.7 ± 0.8	1.00 ± 0.07
48	-83.5 ± 3.4 *†	0.31 ± 0.08*†	-96.8 ± 0.6	1.17 ± 0.09

Table 1. V_m and I_K at 0 and 48 h for EROMK2- and $EROMK2_{V364D}$-expressing oocytes in the presence of BFA. Symbols indicate $^*P < 0.001$ cf. EROMK2V364D, $^\dagger P < 0.001$ cf. $t = 0$

For −BFA oocytes neither V_m nor I_K altered significantly over 48 h. But as shown in Table 1, BFA caused a marked reduction of activity of EROMK2, but not of the mutant.

We conclude that wild-type EROMK2 is endocytosed from the plasma membrane of *Xenopus* oocytes and that substitution of valine 364 by aspartate renders the protein resistant to endocytosis. These results are consistent with the idea that interaction between the C-terminus of ROMK2 and components of the endocytotic mechanism allows entry of ROMK2 into the endocytotic pathway and such interaction may require a functional PDZ domain.

Moral Z *et al.* (2001). *J Biol Chem* **276**, 7156–7163.

Zeng W *et al.* (2002). *Am J Physiol* **283**, F630–639.

SH is a graduate student supported by the Iranian Ministry of Health and Medical Education and the Arak University of Medical Sciences.

All procedures accord with current UK legislation

PS P109

Aldosterone stimulates a rapid increase in urinary sodium excretion but not urinary HCO_3^- excretion nor pH in the anaesthetised rat

Abolfazl K. Rad, Richard J. Balment and Nick Ashton

School of Biological Sciences, University of Manchester, Manchester M13 9PT, UK

Aldosterone appears to exert rapid effects via non-genomic mechanisms in addition to its classical genomic actions. Contrary to its well known genomic action on urinary sodium reabsorption and potassium excretion, we have previously shown that aldosterone causes a rapid increase in urinary sodium excretion but has no effect on potassium output in the rat *in vivo* (Rad *et al.* 2002). Aldosterone has also been shown to inhibit bicarbonate absorption via a non-genomic pathway in the thick ascending limb *in vitro* (Good *et al.* 2002). Accordingly, the aim of this study was to determine whether aldosterone stimulates rapid changes in urinary bicarbonate excretion and urine pH *in vivo*.

Under Intraval anaesthesia (100 mg kg^{-1} sodium thiopentone), male Sprague-Dawley rats received euvolaemic fluid replacement (2.5 % dextrose) of spontaneous urine output using a servo-controlled system (Burgess *et al.* 1993). After a 3 h equilibration period, control urine and plasma samples were taken, following which half of the animals received aldosterone (42 pmol min^{-1}) for 1 h before returning to dextrose alone for the final hour. Animals were humanely killed at the end of the experiment.

	UV μl min^{-1} $100g^{-1}$	$U_{Na}V$ μmol min^{-1} $100g^{-1}$	$U_{HCO3}V$ μmol min^{-1} $100g^{-1}$
Control group			
control hour	11.9 ± 0.7	0.1 ± 0.01	0.05 ± 0.009
treatment hour	14.8 ± 0.9	0.15 ± 0.02	0.06 ± 0.004
Aldosterone group			
control hour	11.9 ± 1.3	0.1 ± 0.01	0.04 ± 0.004
treatment hour	13.6 ± 1.2	*0.3 ± 0.04	0.08 ± 0.02

Table 1. Urine flow rate (*UV*), sodium excretion ($U_{Na}V$) and bicarbonate excretion ($U_{HCO3}V$) over the hour before and during the hour of aldosterone infusion. Values are means ± S.E.M. Comparisons between the control hour and the treatment hour are shown as $^* P < 0.05$, Student's paired *t* test.

Aldosterone infusion had no effect on urine flow rate, but resulted in a significant ($P < 0.05$), rapid increase in urinary sodium excretion (Table 1). Urinary bicarbonate excretion and urine pH did not change over the hour of aldosterone infusion by comparison with control animals. While these data do not provide evidence that aldosterone exerts a rapid effect on urinary pH and bicarbonate excretion *in vivo*, this possibility cannot be excluded due to potential modification or buffering of the final urine downstream of the thick ascending limb. The natriuresis observed following aldosterone infusion confirms our previous observation (Rad *et al.* 2002).

Burgess WJ *et al.* (1993). *Clin Sci* **85**, 129–137.

Good DW *et al.* (2002). *Am J Physiol* **283**, F699–706.

Rad AK *et al.* (2002). *J Physiol* **544.P**, 112*P*.

All procedures accord with current UK legislation

PS P110

Altered renal calcium handling by the offspring of diabetic rats

Helen Bond, Colin P. Sibley, Richard J. Balment and Nick Ashton

School of Biological Sciences, University of Manchester, Manchester M13 9PT, UK

Offspring from mothers with diabetes mellitus are at risk of altered calcium homeostasis. Using the streptozotocin rat model of diabetic pregnancy, we have previously shown that diabetic mothers show marked hypercalciuria (Birdsey *et al.* 1995). We have also shown that the adult offspring of these rats have, by contrast, reduced urinary calcium output (Hamilton *et al.* 1999; Bond *et al.* 2002). Furthermore, increased calbindin-D_{28K} and plasma membrane calcium-ATPase (PMCA) protein expression in kidneys of diabetic rat offspring has also been observed (Bond *et al.* 2002, 2003). The aim of this study was to establish whether these changes in renal function are apparent in younger animals.

Two rat groups were studied; offspring born to control mothers (OC) and offspring born to streptozotocin-induced diabetic mothers (OD). All rats were fostered at birth to a separate group of control dams. Servo-controlled renal clearance techniques were performed on anaesthetised (Intraval 100 mg kg^{-1}) OD and OC at 4 and 8 weeks of age. Urine samples were taken every 15 min, blood samples every hour and glomerular filtration rate was determined by [^{3}H]inulin clearance. Urinary calcium was measured using atomic absorption spectrophotometry. Animals were humanely killed at the end of the experiment.

	4 weeks		8 weeks	
	OC (n=7)	OD (n=5)	OC (n=6)	OD (n=5)
GFR (ml min^{-1})	0.8 ± 0.1	1.2 ± 0.2 *	0.4 ± 0.1	0.8 ± 0.1 **
UV (µl min^{-1})	48.2 ± 11.0	77.8 ± 9.9 *	10.6 ± 3.8	28.6 ± 3.3 **
$U_{Ca}V$ (µmol min^{-1})	0.06 ± 0.01	0.05 ± 0.01	0.02 ± 0.01	0.03 ± 0.01 **
FE_{Ca} (%)	7.1 ± 2.3	3.9 ± 0.7 **	10.7 ± 3.4	5.0 ± 1.0 **

Table 1. Glomerular filtration rate (GFR), urine flow rate (*UV*), calcium excretion rate ($U_{Ca}V$) and fractional excretion of calcium (FE_{Ca}) in offspring of control (OC) and diabetic (OD) mothers. Values are means ± S.E.M. corrected to 100 g body weight. OC *vs.* OD at either 4 weeks or 8 weeks shown by * $P < 0.05$, ** $P < 0.01$, repeated measures ANOVA.

Both GFR and *UV* were significantly higher in 4 week ($P < 0.05$) and 8 week ($P < 0.01$) OD. No difference in calcium excretion was observed at 4 weeks but there was a significant increase ($P < 0.01$) in $U_{Ca}V$ in OD relative to OC at 8 weeks. However, FE_{Ca} was significantly lower ($P < 0.01$) in OD from both groups.

These data show that altered renal calcium handling is apparent in rats born to diabetic mothers from the age of 4 weeks. The decreased fractional excretion of calcium in OD supports previous observations of increased renal calcium transport proteins in offspring born to diabetic mothers.

Birdsey TJ *et al.* (1995). *J Endocrinol* **145**, 94*P*.

Bond H *et al.* (2002). *J Physiol* **544.P**, 94*P*.

Bond H *et al.* (2003). *Pediatr Res* **53** (suppl.), 27A.

Hamilton K *et al.* (1999). *J Soc Gyn Invest* **491** (Suppl. 6), 172A.

This work was supported by the North West Kidney Research Association.

All procedures accord with current UK legislation

PS P111

Stretch-sensing channels in conditionally immortalised human podocytes

Michael J. Morton*, Peter W. Mathieson†, Moin A. Saleem† and Malcolm Hunter*

** School of Biomedical Sciences, Worsley Building, University of Leeds, Leeds LS2 9NQ, UK and †Academic Renal Unit, University of Bristol, Southmead Hospital, Bristol BS2 8BJ, UK*

The glomerular filtration barrier is composed of the capillary endothelium, basement membrane and podocytes. The precise physiological function of podocytes is unknown, but congenital forms of nephrotic syndrome are associated with mutations of podocyte-specific genes (Pavenstadt *et al.* 2003). In order to gain a better understanding of podocyte function we are examining the electrophysiological properties of a conditionally immortalized human podocyte cell line that incorporates a temperature-sensitive SV40 transgene: when cultured at 37 °C the transgene is inactivated and the cells differentiate and express the specific podocyte proteins: nephrin, podocin and synaptopodin (Saleem *et al.* 2002).

Human podocytes were grown to 70/80 % confluence at 33 °C before thermoswitching to 37 °C. Cells were used at least 14 days after thermoswitching, when full differentiation had taken place. Channels were studied by the patch clamp technique at room temperature in cell-attached and inside-out patches with a K^+-rich pipette solution, and mammalian Ringer solution in the bath. Results are given as means ± S.E.M.

Under the above conditions, two channel types are evident in cell-attached patches, with single channel conductances of 137 ± 18 pS ($n = 7$) and 34.5 ± 1.7 pS ($n = 8$). The 137 pS channel is voltage dependent, with depolarisation increasing P_o. These channels are activated upon excision into the bath solution that contains 2 mM $CaCl_2$. The 35 pS channel is sometimes spontaneously active, but its P_o is markedly increased by the application of negative pressure (−10 to −20 cmH_2O) to the rear of the patch pipette. Concomitant with activation of the 35 pS channel, and where both channel types are present in the same patch, the P_o of the 137 pS channel is also increased.

The conductance, voltage dependence and activation upon excision suggest that the 137 pS channel is the large conductance calcium activated channel, BK (KCNMA1, Vergara *et al.* 1998) – this is supported by the presence of BK-encoding RNA detected by RT-PCR. The identity of the 35 pS channel is unknown, but we imagine that, upon membrane stretch, this channel allows Ca^{2+} to enter the cell, raising the local Ca^{2+} concentration and stimulating BK. The above channels constitute a stretch-sensing mechanism in podocytes and their presence suggests that these cells could respond to changes in filtration pressure.

Pavenstadt H *et al.* (2003). *Physiol Rev* **83**, 253–307.

Saleem MA *et al.* (2002). *JASN* **13**, 630–8.

Vergara C *et al.* (1998). *Curr Opin Neurobiol* **8**, 321–329.

This work was supported by the Wellcome Trust.

PS P112

Functional characterisation of phloretin-inhibitable urea transport in the mouse colon

G.S. Stewart*, R.A. Fenton†, F. Thevenod‡ and C.P. Smith*

** School of Biological Sciences, University of Manchester, Manchester M13 9PT, UK, † Laboratory of Kidney and Electrolyte Metabolism, NHLBI, NIH, Bethesda, MD, USA and ‡ Department of Physiology, Univeristy of Witten-Herdecke, D-58448 Witten, Germany*

Colonic bacteria express a urease enzyme that enables them to use host-derived urea as a nitrogen source (Fuller & Reeds, 1998). We have previously reported the possible role in this host–microbial relationship of facilitative UT-A urea transporters located in the mouse colon, and have identified phloretin-inhibitable urea transport in this tissue (Stewart *et al.* 2002). The aim of this study was to further characterise the urea transport in mouse colon in order to investigate the precise role of UT-A transporters.

Tissue was obtained from humanely killed male adult MF1 mice. Refractive light flux experiments using colonic plasma membrane vesicles confirmed the presence of a significant urea flux ($n = 10$, $P < 0.05$, ANOVA) that was inhibited by 0.1 mM phloretin ($n = 4$, $P < 0.01$, ANOVA). Although a similar flux was observed with glutamate, this was not inhibited by phloretin ($n = 3$, $P > 0.05$, ANOVA). Since UT-B transporters are inhibited by mercury compounds while UT-A proteins are not (Martial *et al.* 1996), the fact that 0.5 mM mercury chloride had no effect on the urea flux ($n = 3$, $P > 0.05$, ANOVA) suggests UT-B proteins are not involved. Immunoblotting experiments confirmed that UT-B proteins were not present in the colonic vesicles, but that 34- and 100-kDa UT-A proteins were present. Immunoblots of serially centrifuged samples of mouse colon also indicated UT-A proteins were found in plasma membrane-containing fractions, while UT-B proteins were restricted to fractions containing intracellular proteins. Our results therefore suggest that the UT-A transporters located in the mouse colon are responsible for the observed phloretin-inhibitable urea flux.

Fuller MF & Reeds PJ (1998). *Annu Rev Nutr* **18**, 385–411.

Martial S *et al.* (1996). *Am J Physiol* **271**, F1264–1268.

Stewart GS *et al.* (2002). *J Physiol* **544P**, 94*P*.

This work was funded by the BBSRC and The Royal Society.

All procedures accord with current UK legislation

PS P113

Expression of mRNA for K^+–Cl^- cotransporters (KCC3a, KCC3b and KCC4) in rat pancreatic islet cells

Sarah L. Davies, Philippe Le-Rouzic, Len Best and Peter D. Brown

School of Biological Sciences, University of Manchester, Manchester M13 9PT, UK

The expression of mRNA for K^+–Cl^- cotransporters (KCC) was examined in rat pancreas.

Rats were killed humanely by an overdose of halothane anaesthetic. RNA was extracted either from whole pancreas (endocrine and exocrine tissue), or from isolated islets (prepared by collagenase digestion, see Miley *et al.* 1997). RT-PCR was performed using specific primers for all of the KCC isoforms (i.e. KCC1, KCC2, KCC3a, KCC3b and KCC4). Products were characterised by nucleotide sequencing.

PCR products, of the appropriate size, were obtained with the primers for KCC1, KCC3b and KCC4 and mRNA isolated from the whole pancreas. Products were obtained neither with primers for KCC2 (neuronal specific isoform) nor with primers for KCC3a. PCR performed on islet mRNA revealed expression of KCC3a, KCC3b and KCC4. The products obtained showed 95 %, 100 % and 96 % identity to the known sequences of KCC3a, KCC3b and KCC4, respectively. Neither mRNA for KCC1 nor mRNA for KCC2 was determined in the islets.

In conclusion, we have provided evidence for the expression of KCC3a, KCC3b and KCC4 mRNA in rat pancreatic islets. KCC1 appears to be expressed in the exocrine pancreas but not in the endocrine pancreas.

Miley HE *et al.* (1997). *J Physiol* **504**, 191–198.

S.L.D. is supported by a MRC Studentship.

All procedures accord with current UK legislation

PS P114

Functional analysis of the mouse Na^+–K^+–$2Cl^-$ cotransporter-1 in *Xenopus laevis* oocytes

E. Delpire and R. England (introduced by Peter Brown)

Department of Anesthesiology, Vanderbilt University Medical Center, Nashville, TN, USA

To study the function of the Na^+–K^+–$2Cl^-$ cotransporter-1 (NKCC1), we inserted the 3.7 kb open reading frame of the mouse NKCC1 cDNA into pBF, a *Xenopus laevis* oocyte expression vector.

Xenopus frogs were anesthetized using 0.17 % tricaine in water. All surgeries were approved by the Vanderbilt University Institutional Animal Care and Use Committee. NKCC1 function was assessed via ^{86}Rb-uptakes in oocytes exposed to isotonic (200 mosmol l^{-1}), hypertonic (260 mosmol l^{-1}), or isotonic-low Cl^- solutions.

Experiments performed 1–6 days post-RNA injection revealed a steady increase of the K^+ flux up to day 4, the time at which the flux reaches a plateau. Injection of various amounts of cRNA ranging from 0.03 to 30 ng revealed saturation at 16 ng. K^+ flux times ranging from 5 to 180 min revealed that the oocyte volume was large enough for the specific activity not to reach equilibrium after a 3 h flux. When measured in isosmotic condition, the ouabain-resistant K^+ flux in water-injected oocytes was relatively small, compared to the flux measured with NKCC1-injected oocytes: 1270 ± 91 (mean ± S.E.M., $n = 20$) *versus* 5057 ± 281 pmol K^+ oocyte^{-1} h^{-1} ($n = 20$), respectively. Under hypertonic conditions, the K^+ flux was markedly activated in NKCC1-injected oocytes ($20\,693 \pm 882$ pmol K^+ oocyte^{-1} h^{-1}, $n = 20$), whereas it was only slightly increased in water-injected oocytes. When the oocytes were incubated for 24 h in 6 mM Cl^- compared to 80 mM, the NKCC1 flux in isotonic solution was increased to $12\,819 \pm 428$ pmol K^+ oocyte^{-1} h^{-1}, $n = 20$. The entire NKCC1-mediated K^+ flux was inhibited by 50 mM bumetanide. When the uptake was performed at temperatures ranging from 10 °C to 34 °C, a sharp increase in hypertonically induced NKCC1 flux was observed between 10 °C and 20 °C, followed by a lesser increase thereafter. This temperature effect, leading to a non-linear Arrhenius plot showing an abrupt change in activation energy around 20–23 °C, suggests a significant effect of lipid phase transition. To examine the role of oxidative stress

on NKCC1 function, we tested the effects of arsenite (1 mM) and ascorbic acid (500 μM). Arsenite completely abolished NKCC1 flux, whereas ascorbic acid showed no effect on NKCC1 function. Finally, the specific inhibitor of the p38 MAP kinase pathway, SB203580, did not affect NKCC1 function, as measured in isotonic, hypertonic, or low Cl^- conditions.

This work was supported by NIH grant NS36758.

All procedures accord with current national and local guidelines

PS P115

Expression of L-type (α1D subunit) and T-type (α1G and α1H subunit) Ca^{2+} channels in epithelial-derived human breast cancer cells (ZR-75-1)

L.M. Ashes, T. Clayton, R.L. McDonald, M.W. Saul and C. Garner

School of Applied Sciences, University of Huddersfield, Queensgate, Huddersfield HD1 3DH, UK

Using the video imaging technique this group has previously reported that regulatory volume decrease (RVD) in ZR-75-1 cells is Ca^{2+} dependent. RVD was inhibited in the absence of external Ca^{2+} and in the presence of voltage-gated Ca^{2+} channel inhibitors, nifedipine (L-type) and flunarizine (T-type; Ashes *et al.* 2002). These results suggested that external Ca^{2+} entered the cell via voltage-gated L- and/or T-type Ca^{2+} channels. In this study, the expression of L- and T-type channels was investigated in ZR-75-1 cells using reverse transcriptase-polymerase chain reaction (RT-PCR). The α1C and α1D are subunits of the L-type Ca^{2+} channel. The α1C subunit is expressed in cardiac muscle and the α1D subunit in the CNS and endocrine cells, where it may have a role in stimulus–secretion coupling. The α1G, α1H and α1I subunits have been cloned and display biophysical and pharmacological properties of native T-type Ca^{2+} channels when overexpressed in *Xenopus* oocytes or HEK-293 cells (Randall & Benham 1999).

Total RNA was isolated using the Promega SV Total RNA isolation system. The purity and yield of the total RNA was determined spectrophotometrically and sample integrity was confirmed by agarose gel electrophoresis. Primer sequences were designed for L-type subunits, α1C and α1D, and T-type subunits, α1G, α1H and α1I, using the primer design program 'Primer3' (www-genome.wi.mit.edu). BLAST (Basic Local Alignment Search Tool; www.ncbi.nlm.nih.gov/BLAST) was used to check for sequence alignment and to ensure minimal homology of the primer sequences with other members of the α1-subunit family. Upstream and downstream primer sequences were designed to anneal in different exons to ensure that if contaminated by DNA, genomic products would be larger than those amplified from RNA. Primers for β-actin (Viana *et al.* 1995) were used as positive control as β-actin is ubiquitously expressed. RT-PCR was carried out using the Promega Access RT-PCR system.

Agarose gel electrophoresis of the total RNA yielded the 28S and 18S ribosomal RNA subunits indicating that the isolated RNA was intact and had not degraded. Using the respective primers, fragments corresponding to the expected sizes for α1D, α1G and α1H subunits were obtained.

These results indicate that α1D, α1G and α1H subunit mRNA is expressed in detectable amounts in ZR-75-1 cells. These data support previous work by this group indicating that both L- and T-type voltage-gated Ca^{2+} channels may play a role in Ca^{2+} entry in these cells.

Ashes LM *et al.* (2002). *J Physiol* **544.P**, 109*P*.

Randall A & Benham CD (1999). *Mol Cell Neurosci* **14**, 255–272.

Viana F *et al.* (1995). *J Membr Biol* **145**, 87–98.

PS P116

Water transport system characteristics of erythrocytes at oxidative stress

Maria N. Starodubtseva* and Sergey N. Cherenkevich†

** Gomel State Medical Institute, Lange str. 5, 246000 Gomel, Belarus and †Byelorussian State University, Scoryny ave. 4, 220050 Minsk, Belarus*

As a rule oxidative stress is induced by reactive oxygen species and reactive nitrogen species. Peroxynitrous acid (HOONO) plays an important role in the development of cell oxidative stress. HOONO can modify the structures of lipids and proteins. The HOONO action targets are aromatic amino acids and cysteine (Radi, 1996). The fraction of such amino acid residues in small molecules and ions transporters is higher than in other proteins for example cytoskeleton proteins. An aquaporin-1 cysteinyl is located in the vicinity of the water pore (De Groot *et al.* 2001). Therefore aquaporin is one of the first targets of HOONO action on cells, and osmotic properties are very sensitive to HOONO action. The purpose of this work is the analysis of erythrocyte osmotic property changes with HOONO action.

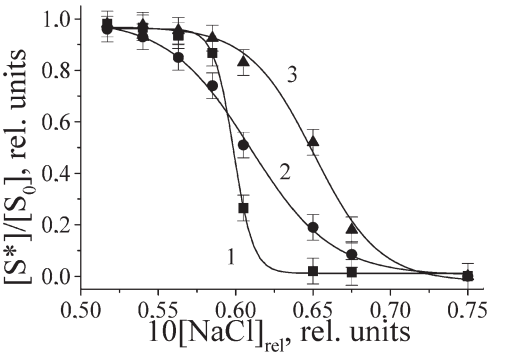

Figure 1. Relative concentration of haemolysed erythrocytes as a function of relative NaCl concentration in a solution. 1, control; 2, erythrocytes treated with 1 mM $NaNO_2$ and H_2O_2; 3, erythrocytes treated with 10 mM $NaNO_2$ and H_2O_2.

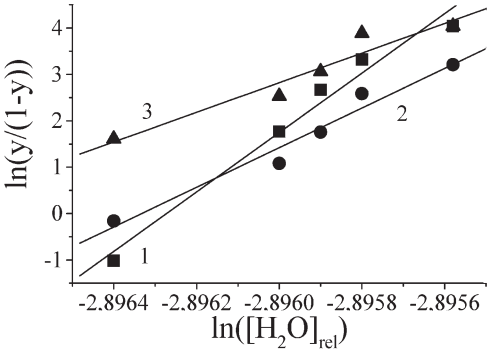

Figure 2. Haemolysis curves in Hill's coordinates. 1, control (r = 6401 ± 903); 2, erythrocytes treated with 1 mM $NaNO_2$ and H_2O_2 (r = 4015 ± 712); 3, erythrocytes treated with 10 mM $NaNO_2$ and H_2O_2 (r = 3187 ± 977). y = [S*]/[S0]

Human erythrocytes from adult donors was obtained at the

Gomel Blood Bank. HOONO was generated directly in erythrocyte suspension by the reaction between $NaNO_2$ and H_2O_2 at equimolar concentrations from 0.025 mM up to 10 mM in acidified solutions (pH 6.3) (Starodubtseva *et al.* 2001). The data were statistically analysed using the one-way analysis of variance ($n = 3–8$, $P = 0.95$).

It was revealed that the dependence of relative haemolysed erythrocyte concentration on relative NaCl concentration (osmolarity) changes with HOONO action (Fig. 1). These changes can be characterized by parameter $b_{50\,\%}$ which is the value of relative NaCl concentration (osmolarity) at 50 % haemolysis and the parameter (r) of cooperativity of the process 'erythrocyte → haemolysed erythrocyte'. The character of the $b_{50\,\%}$ change during oxidative stress is similar to the characters of the changes in lipid peroxidation level and haemoglobin oxidation level (Table 1). The changes of $b_{50\,\%}$ are insignificant at low HOONO concentration up to 1 mM. At high HOONO concentration, rapid growth of parameter $b_{50\,\%}$ is observed. Thus, parameter $b_{50\,\%}$ reflects the accumulation of cell molecule oxidative defects during oxidative stress. The haemolysis curve is in a good agreement with the function $y(x) = x^r/(x^r+D)$, where x is a relative H_2O concentration, r is a cooperativity parameter and D is a constant. According to Hill's full cooperativity theory, this function describes such processes as $[S]+rx \rightarrow [S^*]$. In our case [S] is the erythrocyte concentration, and [S*] is the haemolysed erythrocyte concentration. In this model we consider parameter r as a rate of erythrocyte water transport, that is, the number of water molecules consuming by all erythrocyte aquaporins during one reaction act (10^{-9} s). The analysis of haemolysis curves in Hill's coordinates shows rapid parameter r changes at low HOONO concentration and practically no changes at high HOONO concentration (Fig. 2). So, the parameter r is connected with the coordination of membrane aquaporin acts. At low HOONO concentration, parameter r is a non-monotone function of HOONO concentration (data not presented). That is, the evidence of inbalance in erythrocyte volume regulation system in response to HOONO action.

Concentration of reagents, mM	Intensity of chemiluminescence, relative units	Relative concentration of methemoglobin, %	$10b_{50\%}$, relative units	$b^*_{50\%}$, mOsm
0	11.75±2.78	2±3	0.599±0.001	132.1±9.9
0.05	9.90±5.72	5±4	0.602±0.004	136.5±4.0
0.5	29.90±7.50	18±5	0.603±0.003	137.7±7.4
1	32.90±1.00	43±5	0.609±0.003	140.9±3.7
5	69.00±8.20	98±2	0.639±0.003	152.2±14.2

Table 1. Changes of $b_{50\%}$ ($b5_{0\%}$ is a parameter for a process in aqueous NaCl solution, $b^*_{50\%}$ is a parameter for a process in sodium phosphate buffer), intensity of H_2O_2-induced chemiluminescence of erythrocytes and haemoglobin oxidation during erythrocyte oxidative stress induced by HOONO.

De Groot BL *et al.* (2001). *Science* **294**, 2353–2357.

Radi R (1996). *Method Enzymol* **269**, 354–366.

Starodubtseva MN *et al.* (2001). *Chemiluminescence at the Turn of the Millennium,* pp. 71–75.

PS P117

Characterisation of a novel urea transporter from human colon

E.A. Potter, G.S. Stewart and C.P. Smith

School of Biological Sciences, University of Manchester, Oxford Road, Manchester M13 9PT, UK

Urea movement across plasma membranes is modulated by facilitative transport proteins that are the product of UT-A and UT-B genes. UT-A proteins have been detected in the mammalian colon (Ritzhaupt *et al.* 1998, Stewart *et al.* 2002), where they are proposed to participate in urea nitrogen recycling. We have characterised a 1789-bp cDNA isolated from human colon mucosa encoding a new UT-A isoform (hUT-A6; GenBank Acc. no. AK074236).

hUT-A6 cDNA has a putative open reading frame encoding a 235-amino-acid protein, making it the smallest member of the UT-A subfamily. hUT-A6 is the result of alternative splicing of the UT-A1 gene and contains a novel 127 bp exon between exons 5 and 6. hUT-A6 contains putative consensus PKC phosphorylation sites (Ser15, Ser71, Ser197), but is devoid of putative consensus sequences for PKA phosphorylation. hUT-A6 also contains a putative consensus glycosylation site which lies within the novel exon. The Kyte-Doolittle plot of hUT-A6 suggests this protein shares essentially the same structural configuration as the N-terminal 216-amino acids of hUT-A1, with a hydrophobic core flanked by hydrophilic N-and C-termini.

Xenopus oocyte expression studies were performed as described previously (Smith *et al.* 1995). Expression of hUT-A6 cRNA in *Xenopus* oocytes mediated a significant increase in urea flux, compared to water-injected controls, that was significantly inhibited by 15 min pre-incubation with 0.5 mM phloretin ($n = 8$, $P < 0.05$, ANOVA). hUT-A6-mediated urea flux was significantly increased by 10 min pre-incubated with a cAMP cocktail (0.5 mM cAMP–0.5 mM IBMX–0.05 mM forskolin) compared to unstimulated levels ($n = 8$, $P < 0.05$, ANOVA).

hUT-A6 represents a novel human urea transporter orthalogue and despite its small size, encodes a functional, phloretin-inhibitable facilitative urea transporter similar to other characterised UT-A proteins. Furthermore, this UT-A isoform is positively regulated by a cAMP cocktail despite containing no cAMP-dependent phosphorylation consensus sites, suggesting an alternative intracellular signalling pathway possibly distinct from direct PKA phosphorylation.

Ritzhaupt A *et al.* (1998). *Biochem Soc Trans* **26**, S122.

Smith CP *et al.* (1995). *J Clin Invest* **96**, 1556–1563.

Stewart GS *et al.* (2002). *J Physiol* **544P**, 94*P*.

This work was supported by the BBSRC and the Royal Society.

All procedures accord with current UK legislation

PS P118

P2Y receptor-evoked increases in free cytosolic calcium in human normal and hyperhidrotic sweat glands

S.L. Lindsay*, R. Holdsworth† and D.L. Bovell*

**School of Life Sciences, Glasgow Caledonian University, Glasgow G4 0BA and †Dermatology Department, Stirling Royal Infirmary, Stirling, UK*

The purinoceptor agonist ATP has been shown to induce sweating in the isolated eccrine sweat gland (Sato *et al.* 1994), implicating the P2Y class of receptor in sweat secretion. All P2Y receptor subtypes couple to phospholipase C and hence cause the mobilisation of intracellular calcium (Ca_i^{2+}). We have recently reported that there is an altered distribution of the P2Y receptor subtypes in hyperhidrotic eccrine sweat glands (Lindsay *et al.* 2003), a condition characterised by the production of an inappropriately large volume of sweat. There are no functional data regarding purinoceptors in these abnormal glands. Here we have investigated the increases in $[Ca^{2+}]_i$ elicited by ATP and UTP, in both normal and hyperhidrotic sweat gland cells.

Skin biopsies were obtained with informed consent and local medical ethical committee approval from patients with no apparent skin disease and from those suffering from hyperhidrosis. Freshly isolated glands were obtained using the method of Lee *et al.* (1984) and were cultured and maintained using standard techniques. Primary culture cells grown on glass coverslips were loaded with the calcium-sensitive fluorescent dye, Fura-2 AM (3 μM) for 15 min at 37 °C. The dye was excited at 340 and 380 nm and the fluorescence ratio (340:380) detected at 512 nm. Cells were superfused with Hepes-buffered salt solution (mM): NaCl (130), KCl (5), $MgCl_2$ (1), $CaCl_2$ (1), Hepes (20), glucose (10), pH to 7.4 at 37 °C. Agonists were also diluted in the Hepes-buffered solution. Values are means ± S.E.M. Statistical analyses were carried out using Student's unpaired *t* test, with $P < 0.05$ taken to be significant.

ATP produced a concentration-dependent increase in free cytosolic calcium with a pEC_{50} of 5.32 ± 0.10 in normal cells ($n = 5$) and 5.53 ± 0.10 in hyperhidrotic cells ($n = 4$). In normal cells a maximal concentration of 100 μM ATP evoked an increase in $[Ca^{2+}]_i$ of 0.41 ± 0.05 ratio units ($n = 8$). Hyperhidrotic cells produced an increase of 0.78 ± 0.23 ratio units ($n = 4$) in response to 100 μM ATP, which was significantly greater than normal ($P < 0.05$). In contrast to ATP, UTP was significantly more potent in hyperhidrotic cells, pEC_{50} of 5.78 ± 0.04 ($n = 4$), compared to normal cells, 4.89 ± 0.14 ($n = 5$, $P < 0.001$). In normal cells a maximal concentration of 100 μM UTP caused an increase in $[Ca^{2+}]_i$ of 0.30 ± 0.05 ratio units ($n = 7$), which was significantly less than that found in hyperhidrotic cells, 0.96 ± 0.34 ratio units ($n = 4$, $P < 0.05$).

These results show that in cultured human sweat gland cells there exist purinoceptors that respond to both ATP and UTP, suggesting the presence of at least the $P2Y_2$ receptor subtype. However in cultured hyperhidrotic cells there is a receptor population that is more sensitive to UTP than ATP. Since it is the $P2Y_4$ receptor subtype that is activated preferentially by UTP, it is possible that this receptor has involvement in the excessive sweat production associated with hyperhidrosis.

Lee CM *et al.* (1984). *J Cell Sci* **72**, 259–274.

Lindsay SL *et al.* (2003). *J Physiol* **548.P**, P41.

Sato K *et al.* (1994). In *Pathophysiology of Dermatologic Diseases*, ed. Solter NA & Peterson OH, pp. 211–234. McGraw Hill, New York.

All procedures accord with current local guidelines and the Declaration of Helsinki

PS P119

Calcium homeostasis in identified alveolar epithelial cells: development of a novel *in situ* lung slice model

S. Bourke, H.S. Mason, E.D. Crandall, K.-J. Kim, Z. Borok and P.J. Kemp

School of Biomedical Sciences, University of Leeds, Leeds LS2 9JT, UK and Will Rogers Institute Pulmonary Research Center, University of Southern California, Los Angeles, CA, USA

Of fundamental importance to the optimization of pulmonary gas exchange is the role of the alveolar epithelium in regulation of its micro-environment. In a healthy lung, alveolar efficiency is dependent upon both the degree of hydration and rate of pulmonary surfactant production. Both of these factors are critically regulated by the alveolar epithelial cells. Although much information has been gleaned from isolated cellular studies, little is known about the temporo-spatial relationship of many of the homeostatic processes occurring within an intact epithelium and the impact that intercellular communication has on such processes is currently unknown. Similarly, little information is available on the differential location of key transport proteins within the alveolar epithelium itself. In order to address these controversies we aimed to: (a) to develop a lung slice preparation suitable for physiological study; (b) develop differential live staining of alveolar type I and type II cells within the lung slice; and (c) study Ca^{2+} homeostasis in the identified cells.

Neonatal rats were humanely killed. Lungs were was stabilized by tracheal infusion of 2% agarose followed by immersion in ice-cold, oxygenated solution and then embedded in 4% agarose. Lung slices of 200 μm were processed for live immuno- and histochemical determination of cell localization and viability before being placed in a laser scanning confocal microscope perfusion chamber or being cultured for up to 30 h. Living lung slices were imaged following treatment with a combination of the following reagents: (a) 1:4 mVIIIB2 primary antibody, FITC-labelled anti-mouse IgG secondary (Alveolar type I cells); (b) 1 μg ml^{-1} Nile Red (Alveolar type II cells); (c) 10 μM Hoechst 33342 (live cells); (d) 5 μM propidium iodide (dead cells). $[Ca^{2+}]_i$ was monitored using Fluo-3.

Using this combination of fluorescence histochemistry and immunohistochemistry we have positively identified alveolar type I (VIIIB2) and type II (Nile Red) cells within a living lung slice. Furthermore, we have shown that measurement of dynamic changes of $[Ca^{2+}]_i$ in identified cells within an intact alveolar epithelium is feasible with good temporal and spatial resolution; type II cells demonstrate oscillatory behaviour which is often synchronous and is maintained for up to 30 h in culture. This novel technique will provide the experimental framework upon which to interrogate fully the physiological regulation of the alveolar micro-environment in health and disease.

This work was funded by Wellcome Trust, British Heart Foundation and National Institutes of Health.

All procedures accord with current UK legislation

PS P120

Evidence for Na^+-dependent Cl^-–HCO_3^- exchange in rat brain endothelial cells

C.J. Taylor, S.B. Hladky and M.A. Barrand

Department of Pharmacology, University of Cambridge, Cambridge CB2 1PD, UK

Secretion of fluid into the brain requires transfer of solutes and water across the luminal and abluminal membranes of the endothelial cells lining the brain capillaries. The present study seeks to identify the transporters involved in the movement of Na^+ and/or Cl^- in these endothelial cells by measuring changes in intracellular pH (pH_i).

Brain endothelial cells were grown from isolated rat brain microvessels (rats were humanely killed) and maintained in primary culture. For pH_i measurement, cells were plated on glass coverslips, loaded with BCECF and their fluorescence then measured in a fluorimeter.

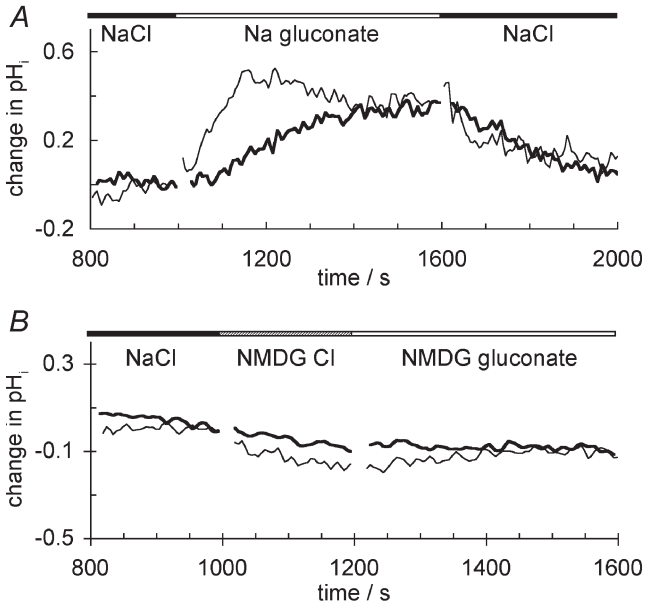

Figure 1. Changes in pH_i following replacement of Cl^- with gluconate$^-$ with (*A*) or without (*B*) prior replacement of Na^+ with $NMDG^+$. Thick trace residual HCO_3^-, thin trace 2 mM HCO_3^- in *A* and *ca* 23 mM in *B*.

Cells in buffer containing 10 mM Hepes and 5 % CO_2/HCO_3^-, pH 7.4 maintained a pH_i of 7.32 ± 0.03 (mean ± S.E.M., $n = 32$) (Taylor *et al.* 2002). Following replacement of Na^+ with $NMDG^+$, a slow progressive acidification was observed with nearly constant rate of decrease in pH_i for at least 600 s. This rate of decrease was similar in the presence or absence of HCO_3^- (0.032 ± 0.002 pH units min^{-1}, $n = 5$ *vs.* 0.027 ± 0.003 pH units min^{-1}, $n = 3$, $P = 0.23$, Student's unpaired *t* test). We reported previously that replacement of Cl^- with gluconate$^-$ in the external buffered solution did not alter pH_i. However, further studies have shown that the effects of replacement of Cl^- depend on the concentrations of Na^+ and HCO_3^- present in the buffer solutions (see Fig. 1). In Hepes buffer containing residual HCO_3^- (estimated as ~100 μM), replacement of external Cl^- by gluconate$^-$ increased pH_i by 0.41 ± 0.03 pH units (mean ± S.E.M., $n = 8$) with $t_{½} = 191 \pm 9$ s (thick trace in *A*). Such a shift is consistent with replacement of total intracellular Cl^- by base equivalents which titrate the intracellular buffers. In Hepes containing 2 mM HCO_3^- the rate of pH_i increase was faster, $t_{½} = 97 \pm 3$ s ($n = 3$), but the extent of the increase was similar (thin trace in *A*). In buffer containing 22 mM HCO_3^-, the response was too fast to resolve ($t_{½} < 10$ s), appearing as a step increase in pH_i (0.15 ± 0.01 pH units, $n = 4$) These are consistent with Cl^-–HCO_3^- exchange as the mechanism of loss of Cl^- and increase in pH_i. When Na^+ was replaced by $NMDG^+$ before withdrawal of Cl^-, the changes in pH_i seen in Na^+-containing Hepes- or HCO_3^--buffered solutions were abolished whether the external solution was buffered with Hepes alone (thick trace in *B*) or with Hepes plus 5 % CO_2/HCO_3^-.

These results indicate the presence of Na^+-dependent Cl^-–HCO_3^- exchange in endothelial cells derived from the rat blood–brain barrier.

Taylor CJ *et al.* (2002). *Pflugers Arch* **443**, s297.

This work was supported by the Sir Jules Thorn Charitable Trust

All procedures accord with current UK legislation

PS P121

The substrate specificity of the human H^+-coupled amino acid transporter (hPAT1) is similar to the imino acid carrier in rat small intestine

D.S. Grenade*, D.J. Kennedy*, M. Boll†, M. Foltz†, S. Miyauchi‡, H. Daniel†, V. Ganapathy‡ and D.T. Thwaites*

**Cell & Molecular Biosciences, The Medical School, University of Newcastle upon Tyne, NE2 4HH, UK, †Molecular Nutrition Unit, Technical University of Munich, Freising-Weihenstephan, Germany and ‡Medical College of Georgia, Biochemistry & Molecular Biology, Augusta, GA, USA*

The substrate selectivities of the 'imino' transporters in rat or rabbit small intestine are distinct (Stevens & Wright, 1985; Munck *et al.* 1994). Little evidence exists for an 'imino' carrier in the human small intestine. cDNAs isolated from rat, mouse and human (Sagne *et al.* 2001; Boll *et al.* 2002; Chen *et al.* 2003) induce, following heterologous expression, H^+-coupled amino (imino) acid transport with identical characteristics to system PAT in human intestinal Caco-2 cells (Thwaites *et al.* 1995). Experiments were designed to determine whether hPAT1 is the human homologue of either the rat imino acid or rabbit IMINO transporter.

Two sets of compounds (1, GABA, β-aminobutyric acid (β-ABA), and α-ABA; 2, isonipecotic, nipecotic and pipecolic acids) were chosen to discriminate between the rat and rabbit systems. Substrate (all 10 mM, pH 5.5, Na^+-free buffers)-induced H^+ flow into BCECF-loaded Caco-2 cell monolayers (passage no. 101–114, 13–29 days post-seeding) (Thwaites *et al.* 1995) and current flow into hPAT1-expressing *Xenopus laevis* oocytes (cRNA 50 ng $oocyte^{-1}$, 3–5 days post-injection) (Boll *et al.* 2002) were determined. The ability of each compound (all 10 mM) to inhibit ^{3}H-labelled *N*-methylaminoisobutyric acid ([^{3}H]MeAIB; 20 μM, 0.5–5 μCi ml^{-1}) uptake (pH 5.5, Na^+-free buffers) via hPAT1 was determined in Caco-2 cells, hPAT1-expressing oocytes or HRPE cells (Chen *et al.* 2003).

A close correlation (linear regression, $r^2 = 0.95$) was observed for each substrate to induce current flow and H^+ flow via hPAT1 in either Caco-2 cells or oocytes. GABA (ΔpH_i min^{-1} 0.119 ± 0.010 (8), mean ± S.E.M. (n)) and β-ABA (0.110 ± 0.011 (8)) both significantly ($P < 0.001$, ANOVA, Bonferroni post test) changed

pH_i whereas α-ABA was without effect ($P > 0.05$). Transported substrates inhibited [^{3}H]MeAIB uptake in each cell-type, e.g. in Caco-2 cells, GABA and β-ABA reduced uptake to 8.2 ± 3.2 (13) and 22.6 ± 2.9 % (14) control (both $P < 0.001$ *vs.* control or α-ABA). The relative ability of substrates to undergo transport or inhibit [^{3}H]MeAIB uptake by hPAT1 is consistent with the predicted pattern for the rat imino acid carrier but distinct from the rabbit IMINO system.

Boll M *et al.* (2002). *J Biol Chem* **277**, 22966–22973.
Chen Z *et al.* (2003). *J Physiol* **546**, 349–361.
Munck BG *et al.* (1994). *Am J Physiol* **266**, R1154–1161.
Sagne C *et al.* (2001). *Proc Natl Acad Sci U S A* **98**, 7206–7211.
Stevens BR & Wright EM (1985). *J Membr Biol* **87**, 27–34.
Thwaites DT *et al.* (1995). *J Membr Biol* **145**, 245–256.

This work was supported by the MRC (G9801704) and BBSRC (13/D17277).

All procedures accord with current UK legislation

PS P122

DMT1 expression in the rat proximal colon is up-regulated by feeding iron-deficient diet

Kelly Johnston and Paul Sharp

Centre for Nutrition and Food Safety, School of Biomedical and Molecular Sciences, University of Surrey, Guildford GU2 7XH, UK

Duodenal iron uptake is mediated by DMT1 at the apical membrane, whilst IREG1 at the basolateral membrane regulates efflux from the enterocyte. However only 10 % of dietary non-haem iron is absorbed in the duodenum, meaning that 90 % reaches the distal region of the small intestine and the colon. Interestingly, a recent report has suggested that, in addition to the duodenum, the proximal colon might also have iron transport capabilities (Bougle *et al.* 2002). To investigate this possibility, we have measured the expression of DMT1 in rat colon. Furthermore, to determine whether colonic DMT1 is regulated by dietary iron intake, we have fed one group of animals on an iron-deficient diet.

Male Wistar rats (250g) were pair-fed for seven days on either control (50 mg Fe kg^{-1}) or Fe deficient (< 0.5 mg kg^{-1}) diet. After this time animals were killed humanely and sections of duodenum, proximal colon and distal colon were removed and subjected to total RNA extraction using the TRIzol method. RT-PCR was performed using DMT1-specific primers and the PCR products resolved on ethidium bromide-stained 2 % agarose gels. Bands were semiquantified using Scion Image software and were normalised to β-actin expression in the same samples.

	DMT1 (IRE)		DMT1 (non-IRE)	
	control	Fe deficient	control	Fe deficient
Duodenum	0.95 ± 0.10 a.u. (8)	1.56 ± 0.25 a.u. (8)*	1.29 ± 0.26 a.u. (4)	2.63 ± 0.70 a.u. (4)
Proximal colon	0.76 ± 0.08 a.u. (8)	1.87 ± 0.45 a.u. (8)*	0.85 ± 0.13 a.u. (4)	1.81 ± 0.44 a.u. (4)*
Distal colon	1.21 ± 0.26 a.u. (8)	1.72 ± 0.50 a.u. (8)	1.95 ± 0.71 a.u. (4)	2.95 ± 1.20 a.u. (4)

Table 1. Effects of iron-deficient diet on DMT1 mRNA expression. Data are means ± S.E.M. of *n* animals in each group. Statistical analysis utilised Student's unpaired *t* test, *$P < 0.05$.

Alternative splicing of exon 16 of the DMT1 gene leads to mRNA variants with differing 3′ untranslated regions (Lee *et al.* 1998) – one contains an iron-responsive element (IRE) whereas the other does not. Following feeding an iron-deficient diet, expression of the DMT1 (IRE) splice variant was significantly increased in duodenum and proximal colon (Table 1). DMT1 (non-IRE) was up-regulated in proximal colon only. Neither splice variant was modulated by iron deficiency in the distal colon. Regulation of DMT1 expression by dietary iron, taken together with our preliminary observations that DMT1 protein is expressed at the cell surface of proximal but not distal colon, supports the hypothesis that the proximal colon under some circumstances could contribute to dietary iron absorption.

Bougle D *et al.* (2002). *Scand J Gastroenterol* **37**, 1008–1011.
Lee PL *et al.* (1998). *Blood Cells Mol Dis* **24**, 199–215.

This work was supported by BBSRC (grant 90/D17146).

All procedures accord with current UK legislation

PS P123

The effects of cobalt on DMT1 protein expression in human intestinal Caco-2 cells

Deborah Johnson and Paul Sharp

Centre for Nutrition and Food Safety, School of Biomedical and Molecular Sciences, University of Surrey, Guildford GU2 7XH, UK

Alternative splicing of exon 16 of the DMT1 gene leads to mRNA variants with differing 3′ untranslated regions (Lee *et al.* 1998) – one contains an iron-responsive element (IRE) whereas the other does not. The relative roles of these splice variants in mediating the intestinal absorption of divalent metals is still unclear. DMT1 can potentially transport a number of metals, including iron (its preferred substrate; Tandy *et al.* 2000), and copper and cobalt (Gunshin *et al.* 1997). Previous studies in our laboratory have shown that both iron and copper regulate transporter protein levels and transport function in Caco-2 cells by selectively down-regulating the expression of the IRE-containing splice variant (Tennant *et al.* 2002; Yamaji *et al.* 2002). To determine whether reduced expression of DMT1(IRE) is a common mechanism by which all potential substrates regulate transporter function we have examined the effects of cobalt on DMT1 protein levels in human intestinal Caco-2 cells using isoform-specific antibodies.

Caco-2 cells were grown for 21 days in 75 cm^2 flasks at which time they are fully differentiated. For the final 24 h cells were incubated in the presence or absence of cobalt (100 μM). Cells were removed from the flask using a cell scraper and used to prepare plasma membranes (Tennant *et al.* 2002) that were subjected to Western blotting using commercially available antibodies (Alpha Diagnostics Inc., USA) against human DMT1 isoforms. The effects of cobalt on a housekeeper protein, villin, were also measured. Cross-reacting bands were semiquantified using Scion Image software and statistical analysis was performed using Student's unpaired *t* test. Data are means ± S.E.M. of 4–6 experiments.

Exposure of Caco-2 cells to cobalt did not alter the expression of the housekeeper protein villin (control 81.4 ± 6.4 a.u.; Co 71.8 ± 10.7 a.u.; $P = 0.54$). Interestingly, the expression of DMT1(IRE) was not significantly different in control and cobalt-treated cells (control 80.0 ± 7.1 a.u.; Co 66.5 ± 7.9 a.u.; $P = 0.28$), whereas the non-IRE isoform was significantly increased following exposure to cobalt (control 35.8 ± 6.6 a.u.; Co 86.8 ± 8.1 a.u.; $P = 0.001$).

Our previous studies with iron and copper suggested that the regulation of DMT1 by its substrates occurred at the post-transcriptional level, perhaps via the interaction of cytosolic iron

regulatory proteins with the IRE in the 3′ untranslated region of DMT1. The mechanism by which cobalt regulates DMT1 expression is unclear and we are currently investigating whether it exerts its influence at the transcriptional or post-translational level.

Gunshin H *et al.* (1997). *Nature* **388**, 482–488.
Lee PL *et al.* (1998). *Blood Cells Mol Dis* **24**, 199–215.
Tandy S *et al.* (2000). *J Biol Chem* **275**, 1023–1029.
Tennant J *et al.* (2002). *FEBS Lett* **527**, 239–244.
Yamaji S *et al.* (2002). *J Physiol* **539.P**, 20*P*.

D.M.J. is supported by a BBSRC Quota Studentship.

PS P124

Analysis of a genetic mutation R177K in Kir6.2 that is responsible for transient congenital hyperinsulinism

J. Mankouri*, A.J. Smith*, H.B.T. Christesen†, K. Brusgaard†, J. Malec†, M. Dunne‡, B. Jacobsen† and A. Sivasprasadarao*

** School of Biomedical Sciences, University of Leeds, Leeds LS2 9JT, UK, † Department of Paediatrics, Odense University Hospital, Denmark and ‡ School of Biomedical Sciences, University of Manchester, Manchester M13 9PL, UK*

Congenital hyperinsulinism (CHI) is a heterogeneous disorder characterised by dysregulated insulin secretion and hypoglycaemia. Central to regulation of glucose-stimulated insulin secretion are the β-cell ATP-sensitive potassium (K_{ATP}) channels. Mutations in the genes encoding β-cell K_{ATP} channels (four subunits each of Kir6.2 and SUR1), which cause a decrease or loss of channel activity, have been shown to produce CHI. Here we have studied the functional and cell biological consequences of a new Kir6.2 mutation, R177K, identified in a female patient suffering from a heterozygous form of CHI.

The mother of the patient was a mild diabetic treated with diet only. The patient had transient, diazoxide-responsive CHI of a severity which could not be explained by the mother's mild diabetes. The patient and mother both possessed a single Kir6.2 mutation, R177K, not seen in > 100 control chromosomes whilst the father presented no mutations. For functional analysis, cRNA encoding the mutant R177K Kir6.2 subunits were coexpressed with SUR1 in *Xenopus* oocytes and channel currents (diazoxide/azide activated, glibenclamide sensitive) were measured by two-electrode voltage clamp. Parallel experiments were carried out with the wild-type Kir6.2. No discernible K_{ATP} currents were observed with the mutant channel ($n = 5$). When sections of these oocytes were immunostained for Kir6.2, no membrane fluorescence was evident, indicating that the mutation prevents trafficking of the channel to the cell surface. Using Kir6.2 containing an engineered extracellular HA epitope, we have investigated the trafficking of the channel to the cell surface in a mammalian cell line. For this, we have co-expressed the HA-tagged Kir6.2 subunits with SUR1 in COS7 cells and examined its cellular localisation by immunoflourescence/confocal microscopy of unpermeabilised and permeabilised cells. The data showed that unlike wild-type Kir6.2, which showed membrane fluorescence, the mutant subunit was almost exclusively localised in the endoplasmic reticulum (ER), as judged by the colocalisation with the ER marker protein calreticulin.

In conclusion, the R177K mutation impairs the trafficking of the K_{ATP} channel to the cell surface. This does not, however, fully account for the transient nature of the CHI. We are currently testing the possibility that the wild-type subunit is able to 'rescue' the trafficking and function of the mutant subunit, thereby accounting for the mild form of CHI presented by the patient with the heterozygous mutation in Kir6.2.

This work was funded by the MRC.

All procedures accord with current UK legislation, local guidelines and the Declaration of Helsinki

PS P125

Inward rectification of the murine two-pore domain K^+ channel TASK-2

Sarah Chipperfield, Michael J. Morton, Asipu Sivaprasadarao and Malcolm Hunter

School of Biomedical Sciences, Worsley Building, University of Leeds, Leeds LS2 9NQ, UK

TASK-2 is a member of the two-pore domain K^+ channel (K_{2P}) family and is sensitive to changes in extracellular pH; currents are maximal at alkaline pH but are progressively inhibited as the pH decreases (Reyes *et al*. 1998). TASK-2 is located principally in epithelial tissues, and is present in all nephron segments (Morton *et al*. 2002). In an unrelated series of whole cell experiments, we noticed that chinese hamster ovary (CHO) cells expressing TASK-2 showed inward rectification which became less pronounced with time, which we supposed was due to loss of an intracellular inhibitor such as a polyamine (Lopatin *et al*. 1994). The following experiments were carried out to determine the basis of this rectification.

Wild-type (WT) murine TASK-2 cDNA was subcloned into the bicistronic vector pIRES-CD8 and transfected into CHO cells using Fugene (Roche). Twenty-four to 72 h post-transfection CHO cells expressing the CD8 antigen were positively identified by incubation with microspheres coated with anti-CD8 antibody (Dynal) and subjected to whole-cell patch clamp analysis. Currents were recorded in either Na^+-rich or Na^+-free (NMDG) mammalian Ringer solution, with a K^+-rich pipette solution which contained different concentrations of the polyamines putrescine (100 μM), spermine and spermidine (up to 1 mM) or Na^+ (5–50 mM). Currents were recorded over the range −100 to +100 mV. Results are given as means ± S.E.M.

In Na^+-free bath solutions the *I–V* curves were linear. Currents were unaffected by the inclusion of any of the polyamines in the pipette solution. However, the inclusion of Na^+ in the pipette solution caused a concentration- and voltage-dependent block of outward currents at positive potentials. Currents at +100 mV were inhibited by: 24 ± 4.4 %, $n = 4$ (5 mM), 39 ± 2.1 %, $n = 7$ (20 mM); and 62 ± 2.2 %, $n = 8$ (50 mM). When the pipette solution was nominally Na^+-free, rectification was reversibly induced by switching between the Na^+-rich and Na^+-free bath solutions.

In conclusion, intracellular Na^+ causes inward rectification of TASK-2 currents. Such rectification is not mimicked by polyamines. The inward leak of Na^+ apparently accounts for all of the rectification observed in conventional whole cell experiments where cells are bathed in mammalian Ringer solution. Since rectification was not induced by polyamines, the mechanism of rectification in TASK-2 is probably different from that of the two transmembrane domain inward rectifier K^+ channels.

Reyes R *et al.* (1998). *J Biol Chem* **273**, 30863–30869.
Lopatin AN *et al.* (1994). *Nature* **372**, 366–369.
Morton MJ *et al.* (2002). *J Physiol* **544.P**, 103*P*.

This work was supported by the Wellcome Trust.

PS P126

Aminoglycoside-induced cell death in calcium receptor-expressing renal cells

D.T. Ward, D. Maldonado-Peres, L. Hollins and D. Riccardi

School of Biological Sciences, University of Manchester, Manchester, UK

Aminoglycoside antibiotics (AGAs) are important in the treatment of life-threatening, Gram-negative infections. However, their clinical usefulness is limited by their otoxicity and nephrotoxicity. To better understand the molecular mechanisms underlying AGA toxicity, we studied their actions in proximal tubule-derived opossum kidney (OK) cells and in human embryonic kidney (HEK) cells stably transfected with the calcium-sensing receptor (CaR). Previously, we have demonstrated that OK cells express the CaR endogenously and that their acute exposure to high extracellular Ca^{2+} levels or to the AGAs neomycin and gentamicin results in intracellular Ca^{2+} mobilisation and phosphorylation of extracellular signal-regulated kinase (ERK) and Akt (Ward *et al.* 2002*a*,*b*). Since such responses are associated with altered cell fate, here we have examined the effect of chronic AGA treatment on OK cell proliferation and cell death.

AGA treatment (500 μM gentamicin) increased OK cell proliferation modestly, but significantly within 24 h as determined by cell counting (+8 ± 2 %; mean ± S.E.M., $n = 7$, $P < 0.01$ by Student's paired t test) and XTT assay (+9 ± 1 %; $n \geqslant 3$, $P < 0.001$ by ANOVA). This is consistent with the acute signalling reported previously (Ward *et al.* 2002*a*,*b*). However, after 4 days' gentamicin treatment there was no evidence of increased cell number, or of G2/M arrest, but instead OK cells underwent dose-dependent cell death as determined using trypan blue (control, 5.5 ± 0.9 % cell-death; gentamicin, 12.6 ± 1.0 %; $n = 7$, $P < 0.01$ by ANOVA) and propidium iodide (flow cytometry). Furthermore, gentamicin elicited significantly more cell death in CaR-HEK cells (control, 2.3 ± 0.1 % cell death; 200 μM gentamicin, 4 ± 0.3 %; 500 μM gentamicin, 6 ± 0.8 %; $n \geqslant 6$, $P < 0.01$ by ANOVA) than in non-transfected HEK-293 cells (control, 1.9 ± 0.1 %; 200 μM gentamicin, 1.8 ± 0.1 %; 500 μM gentamicin, 2.9 ± 0.9 %; $n \geqslant 6$, NS). The size and granularity profiles of the gentamicin-treated cells were comparable for both cell types and neomycin elicited similar effects to gentamicin.

Together these data demonstrate that chronic AGA treatment induces cell death in proximal tubule-derived OK cells. In addition, the presence of the CaR in HEK cells significantly increases their susceptibility to gentamicin-induced cell death raising the possibility that the CaR may itself contribute to AGA nephrotoxicity.

Ward DT *et al.* (2002*a*). *J Am Soc Nephrol* **13**, 1481–1489.

Ward DT *et al.* (2002*b*). *J Physiol* **543P**, 67*P*.

This work was supported by the National Kidney Research Fund (TF6/2002).

PS P127

Effect of the C185S mutation on the Hg^{2+} sensitivity of a frog urea transporter (fUT)

G.J. Cooper

Dept of Biomedical Science, University of Sheffield, Western Bank, Sheffield S10 2TN, UK

Recently a urea transporter (fUT) was cloned from frog urinary bladder (Couriaud, 1999). This transporter shares many properties with the mammalian UT-A family but unlike the UT-A isoforms, fUT is inhibited by the mercurial pCMBS. A sequence alignment comparison of fUT with mUT-A2 and mUT-A3 highlighted a Cys residue C185, which is absent from mUT-A2 and mUT-A3. The aim of the current study was to establish if C185 is linked to the sensitivity of fUT to mercurials, and whether substituting Cys residues into the equivalent positions in mUT-A2 and mUT-A3 imparts mercurial sensitivity to these transporters.

Oocytes were isolated from humanely killed *Xenopus* laevis, and injected with 1 ng (0.02 ng nl^{-1}) cRNA encoding the appropriate urea transporter, its mutant or 50 nl of H_2O. Point mutations were introduced using a PCR-based protocol (Quikchange, Stratagene) and verified by sequencing (Lark Technologies). Uptake of urea into UT-expressing oocytes was performed as described previously (Fenton, 2000). Oocytes were pre-incubated in ND96 containing 0.5 mM $HgCl_2$ for 5 min before uptake. Statistical analysis was performed using Student's unpaired t test or one-way ANOVA coupled with Tukey's test. Statistical significance was assumed at the 5 % level.

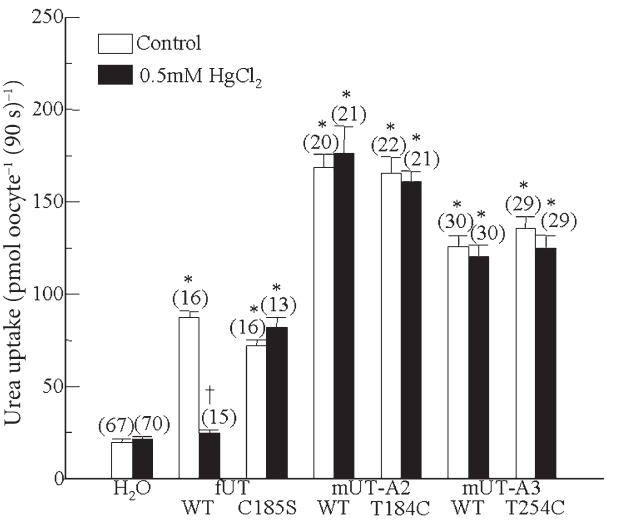

Figure 1. Effect of Hg^{2+} on urea uptake. The uptake period was 90 s using a solution containing 1 mM urea. Values are presented as means ± S.E.M., with the number of observations in parentheses. * denotes a significant increase in uptake compared to H_2O-injected controls. † denotes a significant reduction compared to the paired control group.

Oocytes expressing cRNAs encoding fUT, mUT-A2, mUT-A3 or their mutants exhibited a significant increase in urea uptake compared to H_2O-injected oocytes (Fig. 1). In oocytes expressing fUT, Hg^{2+} reduced urea uptake compared to the paired control group (Fig. 1). In oocytes expressing the fUT-C185S mutant, Hg^{2+} no longer reduced urea uptake (Fig. 1). Cys residues were introduced into the equivalent positions in mUT-A2 (T184C)

and mUT-A3 (T254C). The wild-type mUT-A2, mUT-A3 and the Cys mutants were insensitive to Hg^{2+} (Fig. 1).

These results indicate that C185 plays a role in the sensitivity of fUT to mercurials, implying that this residue lies near the transporter pore. The lack of effect of Cys mutations in mUT-A2 and mUT-A3 suggests either that the effect of Hg^{2+}involves more than one residue, or that differences in the folding of mUT-A2 and mUT-A3, prevent Hg^{2+} binding.

Couriaud C *et al.* (1999). *Biochim Biophys Acta* **1421**, 347–352.

Fenton RA *et al.* (2000). *Am J Physiol* **279**, C1425–C1431.

The support of the Royal Society is gratefully acknowledged. fUT was a gift from P.Ripoche (Saclay, France). mT-A2 and mT-A3 were kindly provided by C. Smith (Manchester, UK).

All procedures accord with current UK legislation

PS P128

Electrogenic HCO_3^- transport across the luminal membrane of guinea-pig pancreatic duct cells

H. Ishiguro, M.C. Steward*, S.B.H. Ko, A. Yamamoto, T. Kondo, R.M. Case*, M. Kitagawa and S. Naruse

*Internal Medicine and Human Nutrition, Nagoya University Graduate School of Medicine, Nagoya, Japan and * School of Biological Sciences, University of Manchester, Manchester, UK*

The interlobular ducts of guinea-pig pancreas secrete HCO_3^- into a HCO_3^--rich (125 mM) luminal fluid following secretin stimulation (Ishiguro *et al.* 1998). Under these conditions intracellular HCO_3^- ($[HCO_3^-]_i$) is ~20 mM and intracellular potential is ~−60 mV (Ishiguro *et al.* 2000, 2002) indicating that there is a luminally directed electrochemical gradient for HCO_3^-. To examine whether luminal HCO_3^- transport is mediated by an anion conductance, we measured changes in intracellular pH (pH_i) when the cells were de- or hyperpolarized by manipulation of extracellular K^+.

Female Hartley guinea-pigs (350–450 g) were humanely killed by cervical dislocation and the interlobular ducts isolated from the pancreas by collagenase digestion and microdissection (Ishiguro *et al.* 1998). pH_i was measured with 2′,7′-bis(2-carboxyethyl)-5(6)-carboxyfluorescein (BCECF). The ducts were superfused with HCO_3^-/CO_2-free Hepes-buffered solution (140 mM Cl^-) and luminally perfused with 125 mM HCO_3^-, 24 mM Cl^-, and 5 % CO_2. Dihydro-4,4′-diisothiocyanatostilbene-2,2′-disulphonic acid (H_2DIDS, 500 μM) was used to inhibit HCO_3^- efflux across the basolateral membrane. Changes in the bath K^+ concentration ($[K^+]_B$) were achieved by replacement with *N*-methyl-D-glucamine and $[Na^+]_B$ was fixed at 60 mM. Tests for statistical significant differences were made with Student's *t* test for paired data.

When $[K^+]_B$ was raised from 5 to 70 mM to depolarize the cells, pH_i in the unstimulated ducts changed only slightly. In the presence of dibutyryl cAMP, which stimulates HCO_3^- secretion, depolarization caused a large increase in pH_i from 6.83 ± 0.11 to 7.32 ± 0.09 (means ± S.E.M., $n = 4$, $P < 0.01$). When $[K^+]_B$ was reduced from 5 to 1 mM to hyperpolarize the cells, pH_i decreased by 0.11 ± 0.01 ($P < 0.05$). To deplete intracellular Cl^-, the ducts were perfused with Cl^--free solutions (containing glucuronate) and stimulated with dibutyryl cAMP for 30 min. Under Cl^- free conditions, when $[K^+]_B$ was reduced from 5 to 1 mM and then raised to 70 mM, pH_i decreased from 7.15 ± 0.06 ($n = 4$) to 7.06 ± 0.07 ($P < 0.05$) and then increased to 7.54 ± 0.16 ($P < 0.01$).

In summary, de- and hyperpolarization caused changes in pH_i that most probably reflected the influx and efflux of HCO_3^- across the luminal membrane. These HCO_3^- movements were not dependent on the presence of Cl^- and may be attributed to the presence of a significant HCO_3^- conductance at the luminal membrane as we have previously suggested (Ishiguro *et al.* 2002).

Ishiguro H *et al.* (1998). *J Physiol* **511**, 407–422.

Ishiguro H *et al.* (2000). *J Physiol* **528**, 305–315.

Ishiguro H *et al.* (2002). *J Gen Physiol* **120**, 617–628.

This work was supported by the Japanese Ministry of Education, Science, Technology, Sports and Culture.

PS P129

Resolution of the insect ouabain paradox

L.S. Torrie*, J.C. Radford*, A.J. Dinsmore†, F.G.P. Earley‡, S.A. Davies* and J.A.T. Dow*

** Division of Molecular Genetics, IBLS, University of Glasgow, Glasgow G11 6NU, † Syngenta, Alderley Park, Macclesfield, SK10 4TJ and ‡ Syngenta, Jealott's Hill International Research Centre, Bracknell RG42 6EY, UK*

The Na^+,K^+-ATPase plays a key role in animal cells; however, many insects are refractory to the Na^+,K^+-ATPase inhibitor ouabain. In *Drosophila* Malpighian (renal) tubules ouabain is almost without effect (Dow *et al.* 1994; Linton & O'Donnell, 1999), although tubules contain Na^+,K^+-ATPases and the *Drosophila* Na^+,K^+-ATPase is ouabain sensitive *in vitro* (Lebovitz *et al.* 1989). We proposed that Malpighian tubules contained a ouabain transport system that protected the Na^+,K^+-ATPase. In vertebrates organic anion transporting polypeptides (OATPs) have broad substrate specificities and can, therefore, transport and eliminate a wide variety of structurally unrelated compounds, including cardiac glycosides.

We adopted a functional genomic approach and screened the *Drosophila* genome *in silico*, identifying eight genes similar to vertebrate OATP members. RT-PCR and *in situ* hybridisation analysis reveal that six of these are expressed in *Drosophila* Malpighian tubules. Fluid secretion assays (Dow *et al.* 1994) reveal that tubule sensitivity to ouabain can be unmasked by competition with alternative transporter substrates, such as taurocholate, sulphobromophthalein (BSP), prostaglandin E_2 (PGE_2) and phenol red (but not cyclic nucleotides). In support of our model, tubules actively transport radiolabelled ouabain, and this can again be inhibited by the addition of alternative transporter substrates. Heterologous expression of the putative *Drosophila* OATPs in NIH3T3 cells reveal that some members of this transport family can transport radiolabelled ouabain and may, therefore, be important in the excretion of ouabain through the Malpighian tubule.

These data show that the Na^+,K^+-ATPase may be as significant in insect tissues as in vertebrates, but is protected by a potent transport system that excretes a range of xenobiotics.

Dow JAT *et al.* (1994). *J Exp Biol* **197**, 421–428.

Lebovitz RM *et al.* (1989). *EMBO J* **8**, 193–202.

Linton SM & O'Donnell (1999). *J Exp Biol* **202**, 1561–1570.

The support of the BBSRC and Syngenta is gratefully acknowledged.

PS P130

Arginine$_{282}$ is a key residue in the proton-coupling mechanism of the rabbit peptide transporter PepT1 expressed in *Xenopus laevis* oocytes

D. Meredith

Department of Human Anatomy and Genetics, South Parks Road, Oxford OX1 3QX, UK

The epithelial di- and tri-peptide transporter PepT1 couples substrate and proton movement in such a way that transport is powered both by the physiological proton gradient across the apical membrane and by the membrane potential (Temple *et al.* 1995). Previously, uptake of the neutral dipeptide D-Phe-L-Gln into R282E-PepT1-expressing oocytes at pH_{out} 5.5 had revealed a functional transporter (Meredith, 2003), which has now been further characterised. Here we report that the site-directed mutagenesis of this arginine residue abolishes the proton coupling of peptide transport.

Arginine$_{282}$ in rabbit PepT1 was mutated to a glutamate using a PCR-based protocol (Quikchange, Stratagene) and confirmed by DNA sequencing to produce R282E-PepT1. Uptake experiments into PepT1-expressing *Xenopus laevis* oocytes were performed as previously described (Meredith *et al.* 2000). Data are means ± S.E.M.

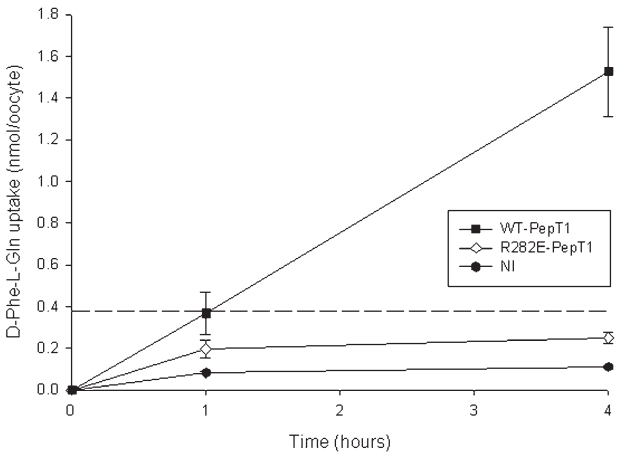

Figure 1. Time course of uptake of ^{3}H-D-Phe-L-Gln into *Xenopus* oocytes expressing wild-type PepT1 (WT-PepT1), R282E-PepT1 or control (NI). No correction has been made for protein expression level. The dashed line represents equilibration assuming an intracellular volume of 1 μl per oocyte. Each data point is the mean ± S.E.M. of 5 oocytes.

Uptake of D-Phe-L-Gln into oocytes expressing R282E-PepT1 was found to be unaffected by extracellular acidification (1.1 ± 0.4-fold increase, $n = 2$), unlike for the wild-type PepT1, which was stimulated by reducing pH_{out} from 7.4 to 5.5 by 2.4 ± 0.3-fold ($P < 0.05$, Student's paired t test, $n = 4$). To investigate whether this was due to peptide uptake no longer being coupled to the proton electrochemical gradient, the ability of the oocytes to perform concentrative uptake at pH_{out} 5.5 was measured, as shown in Fig. 1. As can be seen, R282E-PepT1-expressing oocytes were not able to concentrate D-Phe-L-Gln, unlike those expressing WT-PepT1 which achieved approximately 4-fold concentration above the extracellular level after 4 h.

Taken together, the data that D-Phe-L-Gln uptake by R282E-PepT1 is not stimulated by external acidification nor can R282E-PepT1-expressing oocytes concentrate dipeptide above the external concentration strongly suggest that the proton and dipeptide translocation have been uncoupled, and that R282E-PepT1 behaves as a facilitated diffusion system.

Meredith D *et al.* (2000). *Eur J Biochem* **267**, 3723–3728.

Meredith D (2003). *J Physiol* **549.P**, C7.

Temple CS *et al.* (1995). *Pflugers Arch* **430**, 825–829.

This work is generously funded by the Wellcome Trust.

All procedures accord with current UK legislation

PS P131

Influence of aldosterone and angiotensin II on adaptation of rat colon to low sodium diet

Miquel Moretó, Iram Afzal, Concepció Amat, Anna Pérez-Bosque and Richard J. Naftalin*

*Departments of Physiology, Facultat de Farmacia, Universitat de Barcelona, Spain and *King's College London, Guy's Campus, London, UK*

The functional changes in rat colon on transition from high sodium (HS) diet (4500 μmol NaCl per day) to low sodium (LS) diet (35 μmol NaCl per day) involve decreased crypt wall permeability to 10 kDa dextran and increased Na^+ accumulation from (HS) 144 ± 4 mM (mean ± S.E.M., $n = 4$) to 285 ± 7 mM (LS after 3 days) (mean ± S.E.M., $n = 4$) in the pericryptal sheath. There are also trophic changes in the pericryptal myofibroblastic sheath within 3 days of transition from HS to LS diet (Naftalin *et al.* 2003). We now observe the effects of the angiotensin converting enzyme inhibitor captopril, the angiotensin II receptor type I inhibitor losartan and the aldosterone antagonist spironolactone.

The effects of the following treatments were studied on Sprague-Dawley rats (190–220 g) fed a HS diet for 8–9 days then switched to a LS diet for 3 or 5 days: (a) captopril at 80 mg kg^{-1} day^{-1}; (b) losartan at 30 mg kg^{-1} day^{-1}; and (c) spironolactone at 30 mg kg^{-1} day^{-1}. Drug administration commenced 2 days before switching to a LS diet. [Na^+] in isolated rat distal colonic mucosa was determined by confocal microscopy using a low affinity Na^+-sensitive dye (Sodium Red, and BODIPY) bound to polystyrene beads (Jayaraman *et al.* 2001). Crypt permeability to dextran was monitored by the rate of escape of FITC-labelled dextran (10 kDa) from the crypt lumen into the pericryptal space at 37 °C. Experiments were approved by the Ethical Committee of the University of Barcelona.

The effects of captopril, losartan and spironolactone were confirmed by the significant increases in urinary volume and Na^+ excretion they cause during adaptation to LS diet. Urinary excretion rate of aldosterone (AER) was raised from 50 pmol day^{-1} in HS-adapted animals to 180 pmol day^{-1} in the LS-fed rats. Captopril and losartan decreased AER and spironolactone caused a large increase in AER. All three treatments prevented the increase in myofibroblast growth, already seen after 3 days in LS diet, as shown by the 70–80 % decrease in smooth muscle actin content of the pericryptal sheath myofibroblast smooth muscle actin content in drug-treated animals compared with untreated rats. The increase in pericryptal [Na^+] and decrease in crypt dextran permeability seen 3 days after adaptation to LS diet were also reduced by all drug treatments. The similar nullifying effects of the drugs assayed on adaptation from HS to LS indicate that aldosterone and angiotensin II have linked effects at least on the trophic response of the colon to the LS diet.

Jayaraman S *et al.* (2001). *J Clin Invest* **107**, 317–324.
Naftalin *et al.* (2003). *J Physiol* **548.P**, O82.

This work was supported by The Wellcome Trust.

All procedures accord with current national and local guidelines

PS P132

Inhibition of adenosine transport by gestational diabetes is associated with reduced expression of equilibrative nucleoside transporter 1 and activation of protein kinase C, mitogen-activated protein kinases and nitric oxide synthase in human umbilical vein endothelium

Paola Casanello*†, Felipe Sanhueza* and Luis Sobrevia*

**Cellular and Molecular Physiology Laboratory* (*CMPL*), *Department of Obstetrics and Gynaecology & Medical Research Centre* (*CIM*), *School of Medicine, Pontificia Universidad Católica de Chile, PO Box 114-D, Santiago, Chile and* †*Department of Obstetrics and Gynaecology, Faculty of Medicine, University of Concepción, Chile*

Activity of the human equilibrative nucleoside transporter 1 (hENT1) (sensitive to inhibition by nanomolar nitrobenzylthioinosine, NBMPR) is down-regulated in human umbilical vein endothelial cells (HUVECs) isolated from pregnancies with gestational diabetes (Sobrevia *et al.* 1994). hENT1 expression and activity is also down-regulated in HUVECs from normal pregnancies exposed to 25 mM D-glucose, an effect associated with increased activity of protein kinase C (PKC), endothelial nitric oxide synthase (eNOS) and mitogen-activated protein kinases (MAPK) p44 and p42 (p42/44^{mapk}) (Montecinos *et al.* 2000; Parodi *et al.* 2002). We now report the involvement of PKC, eNOS and p42/44^{mapk} on expression of human ENT1 in HUVECs from gestational diabetes.

Cells isolated (0.2 μg ml^{-1} collagenase) from normal or gestational diabetic pregnancies (ethics committee approval and informed patient consent were obtained) were cultured in medium 199, containing 20 % bovine sera, 3.2 mM L-glutamine, and 5 mM D-glucose. hENT1 mRNA was amplified by reverse transcriptase-polymerase chain reactions on total RNA extracted (Trizol), and quantified by real time PCR. Cells were also exposed (30 min) to PD-98059 (10 μM, MAPK kinase inhibitor), N^G-nitro-L-arginine methyl ester (L-NAME, 100 μM, eNOS inhibitor), calphostin C (100 nM, PKC inhibitor) or RO-320432 (50 or 100 nM, PKC inhibitor), and phorbol 12-myristate, 13-acetate (PMA, 100 nM, PKC activator). hENT1, eNOS and p42/44^{mapk} protein levels were determined by Western blots. eNOS activity was monitored by measuring L-[^{3}H]citrulline formation from L-[^{3}H]arginine (4 μCi ml^{-1}, 100 μM L-arginine, 30 min, 37 °C).

hENT1 mRNA level was significantly lower (70 ± 12 %, $P < 0.05$, Student's unpaired t test, means ± S.E.M., $n = 8$–17) in diabetic compared with normal pregnancies. In addition, gestational diabetes reduced (47 ± 5 %) hENT1 protein level. Maximal NBMPR-sensitive adenosine transport velocity (V_{max}) in diabetic cells was lower (211 ± 45 pmol (10^6 cells)$^{-1}$ s^{-1}) compared with normal cells (712 ± 83 pmol (10^6 cells)$^{-1}$ s^{-1}), with no significant ($P > 0.05$) changes in the apparent K_m (85 ± 12 and 101 ± 23 μM, for normal and diabetic, respectively). Parallel experiments show that maximal binding (B_{max}) was also reduced ($P < 0.05$) in diabetic (0.7 ± 0.1 pmol (10^6 cells)$^{-1}$) compared with normal pregnancies (2.1 ± 0.2 pmol (10^6 cells)$^{-1}$), with no significant changes in apparent K_d (0.21 ± 0.01 and 0.19 ± 0.02 nM, for normal and diabetic, respectively). Gestational diabetes is also associated with increased PKC activity (4.5-fold), eNOS activity (2.7-fold) and protein (3.1-fold) and mRNA (2.4-fold) levels, and p42/44^{mapk} phosphorylation. The effect of gestational diabetes on hENT1 mRNA, NBMPR binding, and adenosine transport was blocked by calphostin C, PD-98059, L-NAME and RO-320432. Calphostin C, L-NAME and RO-320432, but not PD-98059, blocked the effect of gestational diabetes on eNOS.

These results suggest that reduced adenosine transport induced by gestational diabetes could be due to reduced hENT1 expression, via activation of signalling pathways involving PKC, p42/44^{mapk} and eNOS in HUVECs.

Montecinos VP *et al.* (2000). *J Physiol* **529**, 777–790.
Parodi J *et al.* (2002). *Circ Res* **90**, 570–577.
Sobrevia L *et al.* (1994). *Am J Physiol* **267**, C39–47.

This work was supported by FONDECYT (1030781, 1030607, 7030004, 7030109) and DIUC, University of Concepción (201.084.003-1.0), Chile, and The Welcome Trust (UK).

All procedures accord with current national and local guidelines and the Declaration of Helsinki